Title
Investigation of cellular mechanisms involved in mammalian facultative and constitutive heterochromatin formation

Author
de la Cruz, Cecile C

Publication Date
2006

Peer reviewed|Thesis/dissertation

Investigation of Cellular Mechanisms Involved in Mammalian Facultative and Constitutive Heterochromatin Formation

by

Cecile C. de la Cruz

DISSERTATION

Submitted in partial satisfaction of the requirements for the degree of

DOCTOR OF PHILOSOPHY

in

Cell Biology

in the

GRADUATE DIVISION

of the

UNIVERSITY OF CALIFORNIA, SAN FRANCISCO

This work is especially dedicated to Soledad F. Caringal. A true educator, she encouraged me to pursue my Ph.D., and has been a constant source of inspiration in my life, personally and professionally. Grandma, I give you my heartfelt thanks, for all that you've done and all that you are.

Acknowledgements

I wish to start off by thanking my graduate mentor, Barbara Panning, for her unending support of me and my research during my six years in her lab. She has been a nuturing presence in my life and I am grateful for the positive role she has played in my development as a scientist and as an adult.

Gail Martin and Brian Black have been instrumental in my growth as a scientist and I thank them for taking a genuine interest in my career as well as serving on my thesis committee. Ellen Carpenter was my first scientific advisor and exposed me to the joys of scientific discovery.

The past and present members of the Panning Lab have made my days as a graduate student fun, challenging, and thought-provoking. They were my surrogate family. As is true in all families, the Panning Lab has had our share of ups and downs, but all in all these people have enriched my graduate school experience. Thank you for sharing your scientific knowledge, enthusiasm, and laughter with me.

I want to acknowledge all of the special people who brought levity to my life when things were heavy. To my classmates, 'close' co-workers (that's you: Meter, JS), the Bay Area-based crew (Em, Rob, Rose), Margaret Psara, Jocelyn Chung, and childhood friends: your friendships have made me a whole, complete person. Through the hilarity I've even managed to take away a few lessons and nuggets of advice from each and every one of you.

The Caringal and de la Cruz families are a wonderful group who have celebrated every achievement with me. Thank you to my many Aunties, Uncles, and cousins who keep me in their thoughts and prayers. Together we are the American dream realized. I

also am indebted to my Grandpa Lino, Grandma Trining, Grandpa Ven, and Grandma Glory for their love and sharing their unique perspectives on life.

To recount the ways that Dad Oscar, Mom Josie, and bro Cris have supported me would take up as many pages as an entire thesis. Suffice it to say that these three people are very dear to me. Our bond is quite unique, unlike any that I've observed in any other family. I've been blessed many times over, but especially because I was raised by such loving and supportive people. OJCC is not just the acronym of our first names that we use for correspondence, but its's also a representation of our bond. Individual accomplishments are celebrated between the four of us, in the same way that personal burdens are not carried by one, but by 4.

Perhaps my greatest discovery at UCSF was meeting my best friend, Brian Biehs. A friendship that started through shared common interests has now grown into a lasting, meaningful relationship. Having Brian in my life has enrciched my days as a graduate student: he was my rock when times were turbulent, my loudest cheerleader when I needed support, and a proud partner when I finally succeeded. Thank you, Bri. Here's to our future.

Consider it all joy, my brothers, when you meet with various trials, knowing as you do that this tested quality of your faith works out endurance. But let endurance have its work complete, that you may be complete and sound in all respects, not lacking in anything.

James 1:2-5

Kathrin Plath, Kathleen Worringer, Dmitri Nusinow, Matthew Simon, Antonis Kirmizis, and Jia Fang have all contributed to work in this thesis. The 2nd chapter of this work and its accompanying figures were originally published in *Chromosoma*, volume 114(3), pages 183-92. The original publication is available at www.springerlink.com. DOI 10.1007/s00412-005-0008-6.

Abstract

Investigation of Cellular Mechanisms Involved in Mammalian Facultative and Constutvie Heterochromatin Formation

Cecile C. de la Cruz

Heterochromatin is the region of the genome that is cytologically condensed and transciptionally inactive. The two types of heterochromatin, facultative and constitutive, differ by their functions within the nucleus as well as their histone modification profiles. What follows is a study of both types of heterochromatin and the histone methylation marks integral in gene silencing. In female mammals, one of two X chromosomes is packaged in facultative heterochromatin by a non-coding RNA, Xist, and the histone modifying activities that Xist recruits. Here I investigate the spatiotemporal expression of the Xist RNA during mammalian development and find that its expression is coincident with the developmental event of cavitation. Secondly, I characterize a Polycomb Group protein that is recruited to the inactive X chromosome by the Xist RNA, Suz12. Suz12 is required for deposition of the histone H3 lysine 27 tri-methylation mark onto the inactive X chromosome. Lastly, the work within this thesis demonstrates that SUZ12 also plays a role in constitutive heterochromatin formation, and is integral for proper histone H3 lysine 9 tri-methylation. Together this thesis work contributes to our understanding of how both facultative heterochromatin and constitutive heterochromatin are regulated.

Table of Contents **Page**

Dedication iii

Acknowledgements iv

Abstract vii

List of Figures and Illustrations ix

General Introduction 1

Chapter 1 4
Xist RNA coating of the X chromosome *in vivo* occurs concomitantly with cavitation

Chapter 2 19
Developmental regulation of Suz12 expression

Chapter 3 46
The Polycomb Group Protein SUZ12 regulates histone H3 trimethylation and HP1α distribution

Concluding Remarks 69

Appendix 75

References 84

List of Figures and Illustrations **Page**

Figure 1. Whole mount *in situ* hybridization for *Xist* RNA. 15

Figure 2. Serial transverse sections of a cavitating embryo. 16

Figure 3. *Xist* RNA expression begins at 5.5dpc. 17

Figure 4. Riboprobe against *Xist* RNA is specific for females. 18

Figure 5. Levels of Suz12 are similar in somatic cells and embryonic stem cells. 38

Figure 6. Levels of Suz12 remain constant throughout stem cell differentiation. 39

Figure 7. Suz12 is enriched on the Xi in differentiating ES cells during the onset of X-inactivation. 40

Figure 8. Distribution of Suz12 in female blastocysts. 41

Figure 9. Differentiating trophoblast stem cells exhibit a transient enrichment of Suz12. 42

Figure 10. Xi-recruitment of Suz12 is dependent on *Xist*. 43

Figure 11. Two patterns of Suz12 distribution in somatic cells. 44

Figure 12. Distribution of SUZ12 and H3-3mK27 in SUZ12 knockdown cells. 45

Figure 13. Distribution of H3-3mK9 and H3-2mk9 in SUZ12 knockdown cells. 64

Figure 14. EZH2 knockdown results in depletion of H3-3mK27 but not H3-3mK9. 65

Figure 15. Distribution of HP1α in SUZ12 knockdown cells. 66

Figure 16. Increase in micronuclei and chromatin bridges in SUZ12 knockdown cells. 67

Figure 17. Distribution of SUZ12 and SUV39H1 in SUZ12 knockdown cells. 68

Figure 18. The phases of X-inactivation temporally correlate with ES

cell differentiation and embryonic development. 74

Figure 19. SUZ12 co-immunprecpitates with H3-3mK9 HMTase activity 81

Figure 20. Association of SUZ12 and SUV39H1. 82

Figure 21. Chromatin immunoprecipitation at beta satellite repeats. 83

GENERAL INTRODUCTION

The role of proper chromatin structure in the cell is two-fold: it ensures faithful chromosome organization and regulates gene expression. The central structural unit of chromatin is the nucleosome, comprised of approximately 146bp of DNA wrapped around a core of 8 histone proteins. Initial analysis of chromatin by electron micrographs demonstrated that there are two types of chromatin, distinguished by their conformation in low and high salt concentrations. Euchromatin is less compacted chromatin and in low salt conditions exists in a 'beads on a string' conformation, with the beads representing the nucleosomes, and the DNA being the string. Later it was shown that euchromatin is the portion of the genome that is transcriptionally active. Heterochromatin contains DNA that is largely transcriptionally silent due to compact and condensed packaging. The degree of condensation dictates the extent by which DNA is accessible to transcriptional machinery. Condensation state is established and maintained by various mechanisms, including the presence of histone variants in nucelosomes, DNA methylation, and covalent modifications on the N-terminal tails of histones.

The addition of methyl groups onto histone tails by histone methyltransferases (HMTases) alters chromatin structure primarily by recruiting histone methyl-binding proteins. This recruitment subsequently results in chromatin compaction and transcriptional repression. While some methylation marks mediate transcriptional activity, my work has focused on the repressive histone methylation marks and their effect on heterochromatin structure.

There are two types of heterochromatin. Constitutive heterochromatin is characterized by an enrichment of histone H3 lysine 9 tri-methylation (H3-3mK9)

deposited by the SUV39H1 HMTase. Pericentric and telomeric regions are enriched with constitutive heterochromatin, where it plays an essential structural role in cells during all points of the cell cycle. Perturbations in chromatin structure in these regions result in chromosomal instability and telomere shortening (Peters *et al.*, 2001; Garcia-Cao *et al.*, 2004). The other type of heterochromatin, facultative heterochromatin, is developmentally regulated and regulates gene expression. Facultative heterochromatin is regulated largely by histone H3 lysine 27 tri-methylation (H3-3mK27). The Polycomb Repressive Complex (PRC) deposits this mark and its core components are the HMTase EZH2, EED and SUZ12.

A classic example of facultative heterochromatin in mammals is the inactive X chromosome (Xi). In female mammals, one X chromosome is packaged in facultative heterochromatin and transcriptionally inactive. The other X chromosome is euchromatic and expressed, ensuring equal expression of one X chromosome in females and males. The non-coding RNA Xist is required for the process of X chromosome inactivation. *Xist* is expressed exclusively from the future Xi and coats the X chromosome from which it is expressed. This coating is the first in a series of events that sets up and maintains the facultative heterochromatin structure of the Xi.

Xist RNA is believed to recruit a variety of chromatin modifying activities to the Xi, one of which is the HMTase activity of the PRC complex. The Panning Lab and others demonstrated that H3-3mk27 is enriched on the Xi (Plath *et al.*, 2003; Silva *et al.*, 2003). Eed and Ezh2 are recruited in an Xist-dependent fashion to the Xi. Furthermore, these two proteins are required for H3-3mK27 on the Xi (Erhardt *et al.*, 2003; Silva *et al.*, 2003).

The following work is a study of facultative heterochromatin within the context of X-inactivation, as well as characterization of a PRC complex member involved in constitutive heterochromatin formation, SUZ12. In chapter 1, *Xist* expression in the developing female mouse embryo is analyzed to determine the timing of X-inactivation. Molecules that might be involved in the initiation of X-inactivation are discussed in chapter 1. The work in chapter 2 characterizes the role of Suz12 in X-inactivation. This work demonstrates that Suz12 is transiently enriched on the inactive X chromosome during the initiation of X-inactivation and that this enrichment is dependent on the Xist RNA. Although Suz12 is an integral component of the PRC complex it is shown that it has different protein expression profile when compared to its complex members. Lastly, experiments described in chapter 3 indicate that SUZ12 also plays a role in constitutive heterochromatin formation. Together this thesis work contributes to our understanding of how both facultative heterochromatin and constitutive heterochromatin are regulated.

CHAPTER 1

XIST RNA COATING OF THE X CHROMOSOME *IN VIVO* OCCURS CONCOMITANTLY WITH CAVITATION

I. Abstract

Regulated alterations in chromatin structure and gene expression are crucial for specifying the thousands of cell types in higher eukaryotes. Yet the signaling pathways that trigger these changes in chromatin organization are poorly understood. X-inactivation in female mammals is initiated by expression of *Xist* RNA and is a developmentally regulated process by which chromosome- wide changes in chromatin structure result in transcriptional silencing. *In vitro*, X-inactivation and the upregulation of *Xist* RNA expression occurs concomitantly with female ES cell differentiation. Such observations have led to the developmental cue hypothesis- the idea that a developmentally regulated signal triggers the process of X- inactivation. However, it is unclear if X-inactivation occurs concomitantly with a major differentiation event *in vivo* during female embryogenesis. I performed *in situ* hybridization analyses of *Xist* RNA expression during mouse development to determine the exact timing of X-inactivation. *Xist* RNA expression occurs concomitantly with the process of cavitation, between 5.0-5.5dpc. These results were surprising because in contrast to ES cells, X-inactivation *in vivo* occurs prior to differentiation of the three germ layers. If the developmental cue theory is correct, then these findings suggest that the signals that control the process of cavitation may also trigger X-inactivation.

II. Introduction

X-inactivation occurs at two stages during embryonic development and is concurrent with the transition from a pluripotent state to a more restricted state (Goto and Monk, 1998). X-inactivation first occurs in the cells of the extraembryonic lineage, which are

derived from the pluripotent cells of the preimplantation embryo, and give rise to the tissues that provide trophic support to the embryo. These tissues undergo imprinted X-inactivation, such that the paternally derived X chromosome is silenced and the maternally derived X chromosome is active. Later in development, there is a second wave of differentiation and X-inactivation in the tissues of embryonic lineages. This inactivation is random: the maternally and paternally- derived X chromosome each have an equal chance of being chosen to remain active. Both types of X-inactivation, imprinted and random, serve as a hallmark of specification from a pluripotent to restricted cell type, suggesting that the signals that induce specification may also induce X-inactivation.

The X-inactivation center on the X chromosome is required to regulate the process of X-inactivation and contains the *Xist* gene (Plath *et al.*, 2002). The *Xist* gene encodes a spliced, polyadenylated, non-coding nuclear RNA that coats the Xi in female somatic cells. Targeted deletions in *Xist* demonstrate that it is necessary for the initiation of X-inactivation in *cis*. Expression of an inducible Xist cDNA transgene from an autosome is sufficient to cause transcriptional silencing of gene lying in *cis*. Upon differentiation, *cis* spread of *Xist* RNA to coat the Xi must occur in order to cause X-inactivation. *Xist* RNA can be detected at the site of transcription by fluorescent *in situ* hybridization (FISH) as a pinpoint signal from both active X chromosomes in undifferentiated female and male embryonic stem (ES) cells and in the inner cell mass of the embryo. Upon differentiation of ES cells, Xist levels dramatically increase in female cells but not male cells. Xist spreads to coat the presumptive Xi, while the active X retains a low-level of Xist expression that is eventually extinguished. The initial coating

and spread of Xist from the X inactivation center is the first of several steps in transcriptional silencing of the X chromosome.

Biochemical analyses of the expression of X-encoded proteins and cytogenetic studies of the X chromosome have revealed that random X-inactivation begins at the onset of gastrulation (Monk and Harper, 1979; Takagi *et al.*, 1982). Embryos carrying an X-linked *lacZ* transgene exhibited a loss of beta-gal activity in individual cells when X-inactivation occurs. Analysis of these embryos suggested that X-inactivation occurs progressively in the developing embryo, and that some tissues inactivate as late as 11.5dpc (Tan *et al.*, 1993). Yet the perdurance of beta-galactosidase protein may inaccurately reflect the onset of X-inactivation and may give a later estimate of the timing of X-inactivation.

The discovery of *Xist* has provided an excellent *in situ* marker to study the timing of X-inactivation in the developing embryo, as the upregulation of Xist and its coating of the X chromosome is the first step in the process of X-inactivation. Because of its essential role in X-inactivation, it is of primary interest to find the developmental cues that regulate the expression of the *Xist* gene. In doing so, we can begin to understand how X-inactivation is regulated during embryonic development. I performed *in situ* hybridization studies in order to determine whether X-inactivation occurs concomitantly with a major differentiation event during female embryogenesis, and to characterize the exact timing of *Xist* expression *in vivo*. The onset of *Xist* RNA expression occurs between 5.0- 5.5dpc. I found that X-inactivation occurs *in vivo* during the process of cavitation, prior to differentiation of the three germ layers. These findings suggest that signals that initiate cavitation may also serve to trigger X-inactivation *in vivo*.

III. Materials and Methods

Histology and fluorescent in situ hybridization (FISH)

Collection and paraffin embedding of embryos was performed essentially as described (Coucouvanis and Martin, 1999). Fluorescent in situ hybridization on paraffin sections was performed as described (Panning *et al.*, 1997), with the following modifications: slides were first dewaxed by 3 xylene washes for 5 minutes each, then taken through an ethanol rehydration series. Following rehydration and one- 5 minute wash with Phosphate Buffered Saline (PBS), slides were treated with Proteinase K (50ug/ml) for 7 minutes at room temperature, washed with PBS for 5 minutes and then fixed for 20 minutes with 4% paraformaldehyde. Slides were then dehydrated by increasing percentage ethanol washes to 100% ethanol and air- dried. Slides were either stored long term at room temperature, or FISH was immediately performed. *Xist* RNA probe was generated as described previously (Plath *et al.*, 2003).

Whole-mount *in situ* hybridization

Whole-mount *in situ* hybridization was performed as described previously (Neubuser *et al.*, 1997) using a riboprobe prepared against exons 1 and 6 of *Xist*.

IV. Results

To characterize the temporal expression of *Xist* in the developing mouse embryo, I performed whole mount *in situ* hybridization studies. *Xist* is highly expressed in female embryos by 12.5 dpc (Figure 1A) and is not expressed in male embryos (Figure 1B). *Xist*

is already expressed in post-gastrulation embryos at 8.5dpc (Figure 1C) and surprisingly, in 6.0dpc embryos that have not yet undergone gastrulation (Figure 1D).

To pinpoint the exact age at which *Xist* is first upregulated in the embryo proper, I isolated embryos at earlier stages of development. In order to visualize *Xist* expression at a single cell level, I sectioned 5.5dpc and 5.0dpc embryos *in utero* and performed FISH for *Xist*. Figure 2 (A-H) shows serial transverse sections through a cavitating embryo. During cavitation, the center cells of the embryo proper undergo apoptosis while the cells surrounding the cavity undergo a cell shape change. The surviving cells of the embryonic ectoderm change from a cuboidal to columnar shape with a clear apical/basal polarity (Figure 2E). The embryonic ectoderm at this point forms a cup-shaped pseudo-stratified epithelium, with the proamniotic cavity in the center (Figure 2D- F). The differentiated cells of the visceral endoderm (an extra-embryonic cell type) that surround the embryo proper have already undergone imprinted X-inactivation and therefore serve as a way of identifying female embryos (Monk and Harper, 1979; Takagi *et al.*, 1982).

FISH for *Xist* RNA on 5.5dpc embryos shows that *Xist* is already expressed in the nuclei of the embryonic ectoderm, as well as the surrounding differentiated cells of the visceral endoderm (Figure 3A and B). In contrast, the pre-cavitated female embryos at 5.0dpc, as identified by *Xist* expression in the extra-embryonic tissue, do not express *Xist* RNA in the cells of the embryonic ectoderm (Figure 3C and D). The *Xist* RNA probe is specific for females because expression is observed in the maternally- derived tissue of the placenta (Figure 4A), and is not detected in male embryos (Figure 4B). Together these results indicate that the onset of *Xist* expression in the embryo proper begins at 5.5dpc.

V. Discussion

In situ hybridization studies demonstrate that *Xist* expression is first detected in the cells of the embryo proper at 5.5 dpc, indicating that random X-inactivation occurs at this developmental stage. The major developmental transition that occurs between 5.0dpc and 5.5dpc is cavitation, the transition of the solid embryonic ectoderm into a cup-shaped pseudo-stratified columnar epithelium that surrounds the proamniotic cavity. This transition is achieved by a combination of differentiation, cell shape changes and apoptosis that are regulated by interactions between embryonic and extra-embryonic tissues and the basement membrane separating these two tissues. The X-inactivation developmental cue theory posits that the molecules mediating these cell changes may also regulate the onset of X-inactivation.

Bone morphogenic protein 4 (BMP4) produced by the embryonic ectoderm promotes differentiation of an extra-embryonic tissue, the primitive endoderm, into visceral endoderm. BMP4, produced in the embryonic ectoderm, and/or BMP 2 produced in the visceral endoderm promote programmed cell death of the inner embryonic ectoderm cells. The outer cells of the embryonic ectoderm survive because they receive a 'rescue signal' through contact with the basement membrane that lies between the embryonic ectoderm cells and the visceral endoderm (Coucouvanis and Martin, 1995, 1999). BMP4/2 may also promote differentiation of the embryonic ectoderm cells that contact the basement membrane into the polarized columnar embryonic epithelium (Coucouvanis and Martin, 1999).

It is possible that BMP4/2 may also promote X-inactivation. To test this hypothesis, one could study cavitation in ES cells that have perturbed BMP signaling. Differentiating ES cells can be cultured to form embryoid bodies (EBs) that mimic many of the early stages of embryo development, including cavitation (Coucouvanis and Martin, 1995). Blocking BMP signaling by expression of a transgene encoding a dominant negative form of BMP receptor IB prevented cavitation of EBs (Coucouvanis and Martin, 1999). One could determine if X-inactivation occurs in cavitating EBs expressing this transgene in female ES cells. If BMP4/2 or the process of cavitation mediates X-inactivation, then it would be expected that X-inactivation would not occur in EBs that lack BMP signaling. Stable female ES cell lines expressing the mutant *Bmpr-IB* transgene (kindly provided by E. Coucouvanis) were created. Further studies with these cell lines were not pursued because attempts to perform FISH for *Xist* RNA on wild-type cavitating EBs were unsuccessful.

Differentiation of the embryonic ectoderm is separable from epithelialization, as initially the embryonic ectoderm exhibits alterations in gene expression, such as upregulation of *Fgf5*, and downregulation of *Rex1* and *Gbx2*, without accompanying morphological alterations (Haub and Goldfarb, 1991; Rathjen *et al.*, 1999). The basement membrane is necessary for cell polarization and cell death but not differentiation of the embryonic ectoderm. EBs that lack a basement membrane due to a homozygous *Lamc1* mutation are not capable of cavitating (Murray and Edgar, 2000). Similarly, *aPKC* mutant embryos exhibit defects in cavitation, such that the epithelial polarity of the embryonic ectoderm may be disrupted (F. Mariani and G.R. Martin, personal communication). It would be of interest to examine *Lamc1* mutant female ES

cells and *aPKC* mutant female embryos to determine if X-inactivation still occurs in EBs/embryos that exhibit normal differentiation but altered morphology of the embryonic ectoderm. Such studies would uncover which process of cavitation is required for X-inactivation to occur: the change in the differentiation status of the cell, or its subsequent epithelialization.

VI. Figure legends

Figure 1. Whole mount *in situ* hybridization for *Xist* RNA. (A and B) *Xist* RNA is expressed exclusively in female (A) and not male (B) 12.5 dpc embryos. Female 8.5dpc embryos (C) and female 6.0dpc embryos (D) also ubiquitously express *Xist*.

Figure 2. Serial transverse sections of a cavitating embryo. Paraffin sections were stained with DAPI to delineate the nuclei. The proamniotic cavity forms via apoptosis of the inner cells of the embryonic ectoderm (C-F). Surviving embryonic ectoderm cells arrange themselves in a columnar epithelium (see inset in E). Differentiated visceral endoderm cells are aligned perpendicular to and surround the embryo proper (see inset in E).

Figure 3. *Xist* RNA expression begins at 5.5dpc. FISH for *Xist* RNA (first column) and DAPI (second column) to visualize the nuclei. The merged image (third column) consists of *Xist* RNA (green) and DAPI (blue). (A and B) Transverse sections of a 5.5dpc embryo. *Xist* is expressed in the columnar cells of the embryonic ectoderm as well as the visceral endoderm. (C and D) *Xist* is only expressed in the visceral endoderm in female pre-cavitated 5.0dpc embryos, but not in the cuboidal shaped cells of the embryonic ectoderm.

Figure 4. Riboprobe against *Xist* RNA is specific for females. FISH for *Xist* RNA (first column) and DAPI (second column) to visualize the nuclei. The merged image (third column) consists of *Xist* RNA (green) and DAPI (blue). Maternally- derived placental

Figure 1

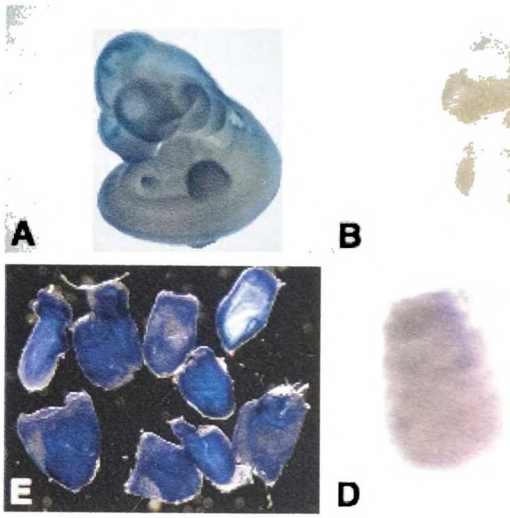

Figure 2

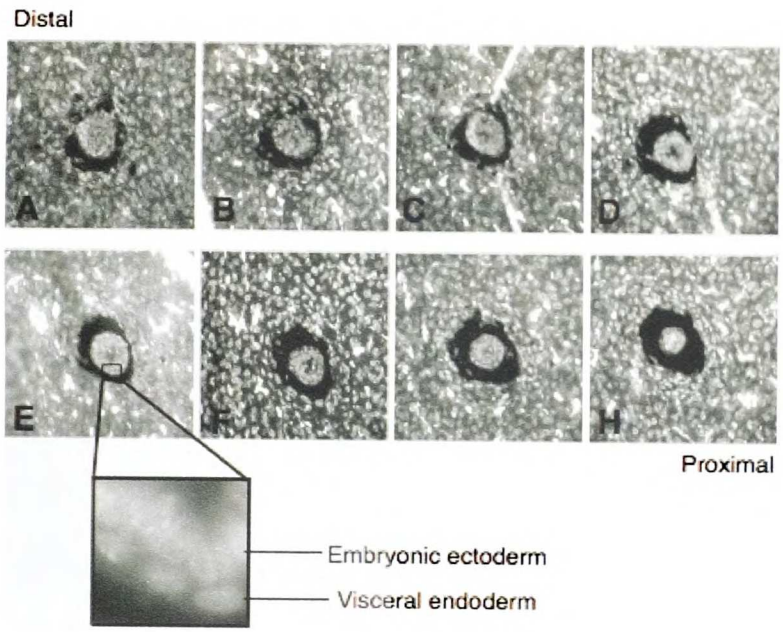
Distal
A
B
C
D
E
F
H
Proximal
Embryonic ectoderm
Visceral endoderm

Figure 3

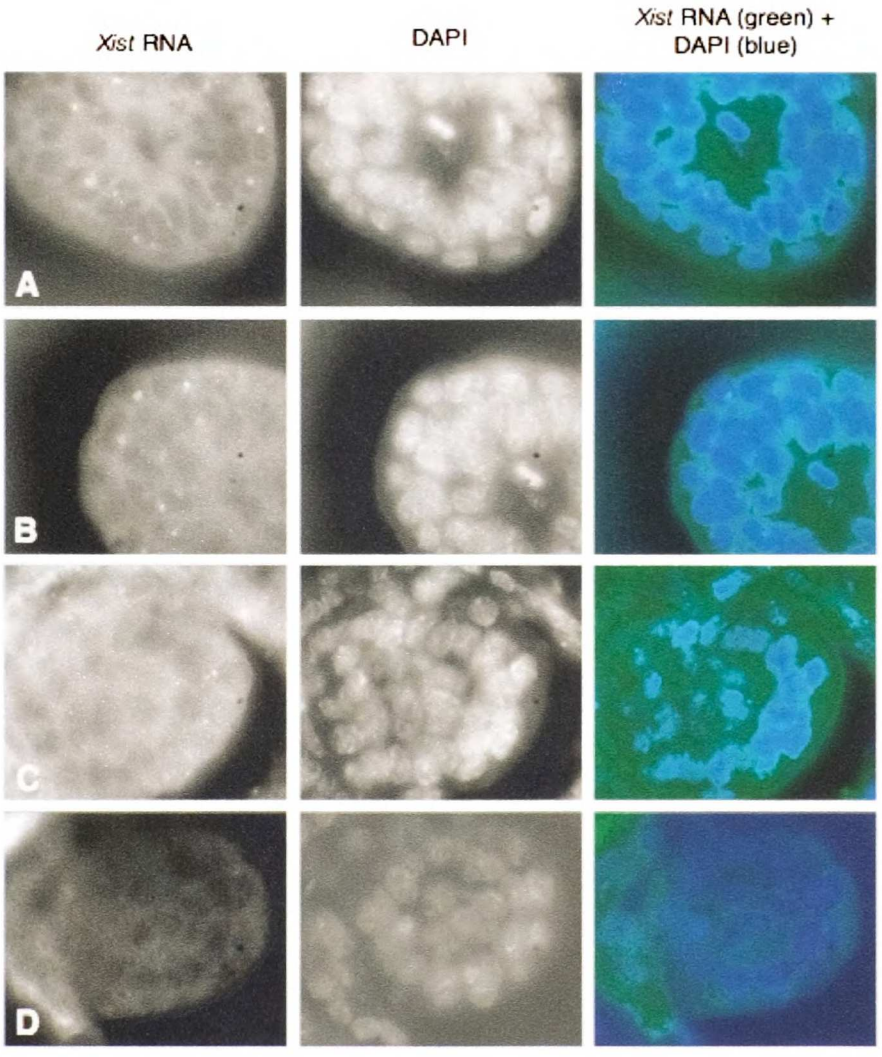

Figure 4

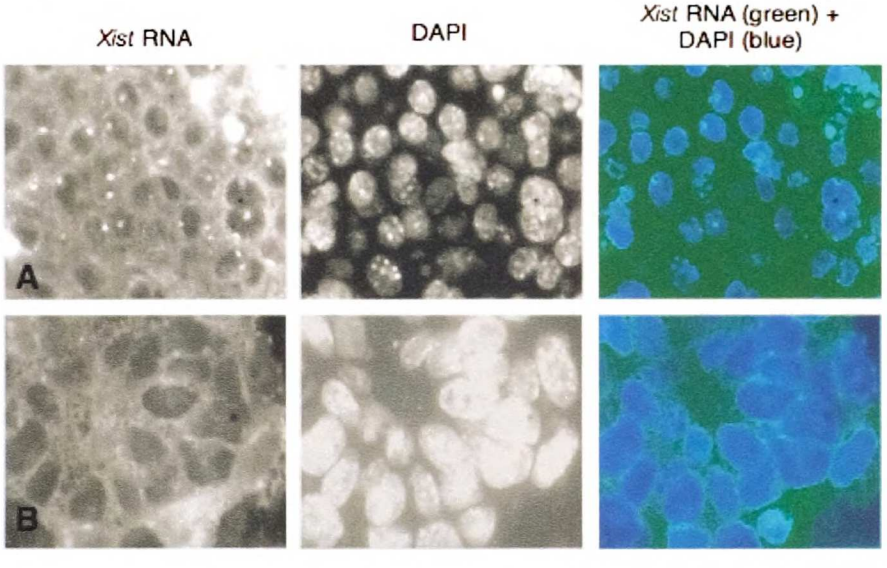

CHAPTER 2

DEVELOPMENTAL REGULATION OF SUZ12 EXPRESSION

I. Abstract

Chromatin modifications are among the epigenetic alterations essential for genetic reprogramming during development. The Polycomb group (PcG) gene family mediates chromatin modifications that contribute to developmentally- regulated transcriptional silencing. Tri-methylation of histone H3 on lysine 27, mediated by a PcG protein complex consisting of Eed, Ezh2 and Suz12, is integral in differentiation, stem cell self-renewal, and tumorigenesis. Eed and Ezh2 are also implicated in the developmentally-regulated silencing of the inactive X chromosome, as they are transiently enriched on the inactive X chromosome when X chromosome silencing is initiated. Here we analyze the dynamic localization of Suz12 during cellular differentiation and X-inactivation. Though Suz12 is a requisite member of the Eed/Ezh2 complexes, we found that Suz12 exhibits a notable difference from Ezh2 and Eed: while Ezh2 and Eed levels decrease during stem cell differentiation, Suz12 levels remain constant. Despite the differential regulation in abundance of Suz12 and Eed/Ezh2, Suz12 is also transiently enriched on the Xi during early stages of X-inactivation and this accumulation is *Xist* RNA dependent. These results suggest that Suz12 may have a function that is not mediated by its association with Eed and Ezh2, and that this additional function is not involved in regulation of X-inactivation.

II. Introduction

Epigenetic gene silencing is critical during development and plays a role in several cell fate processes, including maintenance of pluripotency, differentiation, and cancer progression. In each case, heritable gene silencing by chromatin modifications

contributes to changes in gene expression patterns. Methylation of histone H3 on lysine 27, mediated by Polycomb group (PcG) proteins Eed, Ezh2, and Suz12, has been implicated in transcriptional silencing (Cao *et al.*, 2002; Czermin *et al.*, 2002; Kuzmichev *et al.*, 2002; Muller *et al.*, 2002; Cao and Zhang, 2004b; Kirmizis *et al.*, 2004; Pasini *et al.*, 2004).

Dosage compensation in female mammals serves as an excellent model to study the effects of chromatin modifiers on gene expression, since alterations in the epigenetic landscape of the X chromosome result in the transcriptional silencing of one of the two X chromosomes. X-inactivation occurs twice during mouse embryonic development. The first wave of X-inactivation occurs exclusively on the paternally-inherited X chromosome during pre-implantation development, resulting in imprinted X-inactivation in extra-embryonic tissues (Heard, 2004). X-inactivation in the embryonic tissues occurs after implantation and is random, such that either the paternally- or maternally- inherited X chromosome has an equal probability of being silenced in each cell. Both forms of X-inactivation involve at least two steps: the initial silencing of the inactive X chromosome (Xi) and stable maintenance of the Xi throughout all subsequent cell divisions.

The *Xist* gene encodes a 17 kb non-coding RNA that remains in the nucleus to coat the Xi. When X-inactivation is triggered, *Xist* RNA spreads in *cis* from its site of transcription to cover the Xi (Panning *et al.*, 1997; Sheardown *et al.*, 1997). X chromosomes bearing *Xist* deletions are not silenced, demonstrating that *Xist* is necessary for X-inactivation in *cis* (Penny *et al.*, 1996; Marahrens *et al.*, 1997). Expression of an inducible *Xist* cDNA transgene from autosomes results in *Xist* RNA coating and transcriptional silencing of autosomal genes lying in *cis*, indicating that *Xist* RNA coating

is sufficient for silencing (Wutz and Jaenisch, 2000). *Xist* continues to be transcribed exclusively from the Xi in differentiated female cells, where it plays a minor role in maintenance of the inactive state.

The Xi in somatic cells is characterized by a series of chromatin modifications that distinguish it from the active X chromosome and autosomes. The Xi exhibits enrichment of the variant histone macroH2A, altered levels of histone H3 and H4 methylation, decreased amounts of acetylation on histones H3 and H4, ubiquitination of histone H2A, and an increase in DNA methylation of CpG islands (de Napoles *et al.*, 2004; Fang *et al.*, 2004; Heard, 2004; Smith *et al.*, 2004). These changes in chromatin structure are set up sequentially during the early stages of X-inactivation, indicating that an ordered series of epigenetic modifications may be required to initiate and establish X chromosome silencing (Chaumeil *et al.*, 2002).

The tri-methylated form of histone H3 on lysine 27 (H3-3mK27) is enriched on the Xi during the earliest stages of X-inactivation, suggesting a role in initiation of X chromosome silencing (Plath *et al.*, 2003; Silva *et al.*, 2003). This modification persists on the Xi in some somatic cell types during the maintenance phase (Gilbert *et al.*, 2003). H3-3mK27 accumulation on the Xi is dependent on the PcG proteins Eed and Ezh2, which are transiently enriched on the Xi in differentiating female embryonic cells (Erhardt *et al.*, 2003; Plath *et al.*, 2003; Silva *et al.*, 2003). While *Eed* mutant females initiate X-inactivation normally, perhaps due to abundant maternal stores of Eed, a subset of extra-embryonic cells reactivate their Xi, demonstrating a role for this complex in the maintenance of X-inactivation (Wang *et al.*, 2001; Silva *et al.*, 2003). Although Eed and

Ezh2 play a vital role in the tri-methylation of histone H3 on lysine 27 on the Xi, it is still unknown whether Suz12 is also required for this process.

To better understand the function of Suz12 I analyzed the alterations in its amount and distribution during stem cell differentiation. Eed and Ezh2 levels drop upon differentiation (Silva *et al.*, 2003; Kuzmichev *et al.*, 2005). In contrast, amount of Suz12 remained constant in differentiating stem cells, suggesting a role for Suz12 in addition to the regulation of Eed/Ezh2-mediated histone methylation. While Suz12 differed from Eed and Ezh2 in developmental regulation of abundance, it showed the same transient enrichment on the Xi in differentiating cells as Eed and Ezh2. Enrichment of Suz12 on the Xi required *Xist* RNA. As expected for an essential component of the H3-3mK27 histone methyltransferase complex, knockdown of SUZ12 in human cells results in loss of Xi-enriched and genome-wide H3-3mK27. These data indicate that Suz12 contributes to H3-K27 methylation on the Xi.

III. Materials and methods

Cell culture

Trophoblast stem (TS) cells were kindly provided by Uy et al. (Uy *et al.*, 2002) and cultured as described by Tanaka et al. (Tanaka *et al.*, 1998). To induce differentiation, TS cells were washed with PBS and then cultured in medium without FGF4, heparin, and EMFI-CM. Transformed mouse embryonic fibroblasts, transformed mouse fibroblasts, ES cells, and blastocysts were cultured as described previously (Panning *et al.*, 1997). Analysis of ES cell differentiation was carried out as indicated in Plath et al., 2003. Male ES cells carrying a tetracycline inducible *Xist* gene on the X chromosome, and expressing

the reverse tetracycline-controlled transactivator from the *Rosa 26* locus (Plath et al., 2004) were incubated in the presence of 2 μg/ul doxycyline for 24 hours. The IMR90 human female fibroblasts were purchased from American Type Culture Collection (ATCC, Cat # CCL-186) and cultured according to ATCC's handling procedures.

siRNA transfection

SUZ12 siRNA SMARTpool (M0069570050) and control GFP siRNA oligonucleotides (D0013000120) were obtained from Dhramacon Research Inc. siRNA duplexes were transfected into IMR90 cells using Lipofectamine 2000 (Invitrogen) according to manufacturer's instructions. Transfected cells were incubated with the siRNA for 72 hours, at which time they were harvested and re-plated at the original starting density. Cells were then re-transfected with the oligonucleotides and incubated for an additional 72 hours. Six days after the initial siRNA transfection, the cells were fixed for immunofluorescence as detailed below.

Antibodies

Antibodies against Ezh2, Eed, H3-3mK27, and RbAp48 have been previously described (Cao *et al.*, 2002; Hamer *et al.*, 2002; Kirmizis *et al.*, 2003; Kirmizis *et al.*, 2004). Two different rabbit polyclonal antibodies for Suz12 were used (Abcam; Cao et al., 2002). A chicken Eed serum (Abcam) gave results identical to the mouse monoclonal (Hamer et al. 2002), and was also employed in some instances. In some experiments a mouse monoclonal H3-3mK27 antibody (Abcam) was used.

Immunofluorescence and fluorescence in situ hybridization (FISH)

Immunofluorescence and combined FISH and immunofluorescence were carried out as described previously (Plath et al., 2003). *Xist* RNA was detected with a fluorescein-UTP (Roche) labeled single-stranded RNA probe antisense to mouse *Xist* exon 7. Human *XIST* RNA was detected with a fluorescein-UTP (Roche) labeled single-stranded RNA probe antisense to *XIST* exon 1.

Western Blotting

For Western blots, ES and TS cells were collected, washed and lysed for 2 hours in an appropriate amount RIPA buffer (50 mM Tris-HCl, 150 mM NaCl, 10 mM NaF, 1 mM EDTA, 1 mM Na_3VO_4, 1% NP-40, 0.25% sodium deoxycholate, 0.1 mM PMSF, 0.5 mM DTT, leupeptin, aprotinin, and pepstatin A, pH 7.4). The solution was then clarified by centrifuging at top speed for 15 minutes and supernatant proteins were fractionated in a 12% SDS-PAGE. Blotting was carried out using standard procedures.

IV. Results

Suz12 levels remain constant throughout stem cell differentiation

Eed and Ezh2 levels decrease upon differentiation of embryonic stem (ES) cells (Silva *et al.*, 2003; Kuzmichev *et al.*, 2004). To determine whether Suz12 was also down-regulated during differentiation, we analyzed the amounts of Eed, Ezh2, and Suz12 in undifferentiated ES cells and a transformed fibroblast cell line. Western blot analysis showed that levels of Eed and Ezh2 were very low to undetectable in the fibroblast line and abundant in the undifferentiated ES cells (Figure 5A), consistent with the previously

reported differentiation-induced decrease in abundance of these two PRC2 proteins (Kuzmichev et al. 2004; Silva et al. 2003). Suz12 was present in similar quantities in both cell types (Figure 5A). These results were confirmed by immunostaining for Eed, Ezh2, and Suz12 in undifferentiated ES cells and fibroblasts (Figure 5B-E). We next examined whether levels of Suz12 changed during differentiation of stem cells. During an ES cell differentiation time course, amounts of Ezh2 decreased rapidly upon differentiation, such that by day 6 no protein was detectable (Figure 6A), consistent with the previously reported decrease in Ezh2 and Eed in differentiating ES cells (Kuzmichev et al. 2005; Silva et al. 2003). In contrast, levels of Suz12 remained constant throughout the time course. A stem cell type of the extraembryonic lineage, trophoblast stem (TS) cells, displayed similar dynamics of Ezh2 and Suz12 levels when differentiated (Figure 6C). Ezh2 was virtually absent by day 6 and Suz12 levels remained uniform upon differentiation. These data indicate that developmental regulation of Suz12 expression differs from that of Ezh2 and suggests that Suz12 may carry out functions that are independent of its interaction with Eed and Ezh2.

Suz12 is transiently recruited to the Xi upon initiation of X-inactivation

Eed and Ezh2 are transiently enriched on the Xi during initiation of X chromosome silencing (Plath *et al.*, 2003; Silva *et al.*, 2003), and Suz12 has been detected in cells initiating X-inactivation (de Napoles *et al.*, 2004). As levels of Suz12 remained constant throughout ES cell differentiation, while the levels of Eed and Ezh2 dropped, it suggested that Suz12 might show a temporally distinct pattern of Xi-enrichment during the progression of X-inactivation. To determine whether the kinetics of Xi-localization of

Suz12 differed from that of Eed, we analyzed the localization of Suz12 and Eed in differentiating ES cells. Immunostaining for Suz12 was combined with fluorescence in situ hybridization (FISH) for *Xist* RNA or immunostaining for Eed to mark the Xi. In undifferentiated ES cells that had no *Xist* RNA coating or enrichment of Eed on either of active X chromosomes, Suz12 was distributed uniformly throughout the nucleus (Figure 7A, 7C). When ES cells were induced to differentiate, Suz12 accumulated on the Xi, as marked by *Xist* RNA coating or Eed accumulation (Figure 7B, 7D). By day 2 of differentiation, 97% of cells that had an *Xist* RNA-coated Xi showed Xi –enrichment of Suz12 (Figure 7E). At day 6 of differentiation, 95% of cells that had an *Xist* RNA-coated Xi showed Xi-enrichment of Suz12 or Eed (Figure 7E). The proportion of cells with an *Xist* RNA-coated Xi that displayed Suz12 or Eed enrichment remained steady until day 8 of differentiation and then dropped, so that by day 13 there were no cells with Suz12 or Eed Xi-enrichment. These results indicate that Suz12, like Eed, is transiently recruited to the Xi during initiation of X-inactivation in differentiating ES cells. Since Suz12 levels remain relatively high in differentiated cells, the lack of Xi-enrichment of Suz12 suggests that Suz12 can only accumulate on the Xi when it is present in a complex with Eed and Ezh2.

The enrichment of Eed and Ezh2 on the Xi is transient in extra-embryonic cell types as well (Plath *et al.*, 2003; Silva *et al.*, 2003). To determine whether Suz12 showed the same transient enrichment on the Xi we analyzed the distribution of Suz12 and Eed in cultured blastocysts. Trophoblast giant cells, differentiated extra-embryonic cells derived from the trophectoderm, develop from cultured blastocysts. We observed progressive loss of Suz12 and Eed staining on the Xi in giant cells. Four days after plating, the giant cells

of female blastocysts showed a strong Xi staining pattern of Suz12 and Eed (Figure 8A). After 8 days in culture the Xi staining of Suz12 and Eed were considerably weaker, and many giant cells lacked any detectable staining (Figure 8B). These results demonstrate that Suz12 shows the same dynamic enrichment on the Xi that was previously observed for Eed and Ezh2.

TS cells are an extra-embryonic stem cell type that is derived from the trophectoderm (Tanaka *et al.*, 1998; Kunath *et al.*, 2004). TS cells are unusual in that they are the only cell type that exhibits enrichment of Eed, Ezh2, and H3-3mK27 on the Xi in their undifferentiated state (Mak *et al.*, 2002). When TS cells are differentiated, there is a decrease of Eed, Ezh2 and H3-3mK27 staining on the Xi, and after several days in differentiating conditions, Xi-enrichment of these marks are no longer detected (Plath *et al.*, 2003; Silva *et al.*, 2003). To determine if Suz12 showed the same progressive loss of Xi-enrichment, we performed immunofluorescence for Suz12 on differentiating female TS cells (Figure 9). Undifferentiated TS cells exhibited enrichment of Suz12 on the Xi, shown by co-localization of Suz12 with H3-3mK27 (Figure 9A). Differentiating TS cells showed clear localization of Suz12 and H3-3mK27 on the Xi in all cells at 2 days of differentiation (Figure 9B). There was a gradual decrease in the proportion of cells showing Xi-localization of Suz12, such that by day 4 cells with Xi-enrichment of Suz12 were no longer detected (Figure 9C). H3-3mK27 enrichment on the Xi also decreased over time, and was no longer detectable by day 8 of differentiation (Figure 9E). These results indicate that Xi-enrichment of Suz12, like Xi-enrichment of Eed, Ezh2 and H3-3mK27, is lost upon differentiation of TS cells. Suz12 redistributed from an exclusively uniform nuclear staining pattern with Xi- enrichment (Figure 9A) to accumulate in many

dispersed bright speckles within the nucleus (Figure 9E), suggesting that developmental regulation of Suz12 localization at regions other than the Xi may occur. In addition Suz12 was also detected in the cytoplasm of differentiating TS cells, a distribution that was unique to TS cells.

Suz12 recruitment to the Xi is dependent on Xist RNA

Xi-accumulation of Ezh2, Eed, and H3-3mK27 are dependent on initial coating of the Xi by *Xist* RNA (Plath *et al.*, 2003; Silva *et al.*, 2003). To determine whether Xi-enrichment of Suz12 was also *Xist* RNA dependent, we assayed whether induction of *Xist* expression in undifferentiatied male ES cells was sufficient to recruit Suz12. We employed a cell line in which the *Xist* promoter was replaced by a tetracycline-inducible promoter (Plath *et al.*, 2004). The distribution of *Xist* RNA and Suz12 was assayed in induced and uninduced cells. Uninduced cells did not express *Xist* RNA and did not show any localized enrichment of Suz12 (Figure 10A). After twenty-four hours of induction (Figure 10B), *Xist* RNA coated the X chromosome and Suz12 was also enriched on the X, indicating that *Xist* RNA is sufficient to recruit Suz12 to the Xi. Given that *Xist* RNA is also sufficient to recruit Eed and Ezh2 (Plath et al. 2003), it is likely that Suz12 recruitment to the Xi occurs as a complex with Eed and Ezh2.

Differentiated cell types do not exhibit constitutive Xi-enrichment of Suz12

To determine if Suz12 is localized to the Xi in somatic cells in the maintenance stage of X-inactivation, we stained two female transformed clonal fibroblast cell lines for Suz12 and used FISH for *Xist* RNA to mark the Xi. The majority of these cells exhibited

nuclear speckles of Suz12 that were not uniformly distributed (Figure 11A). Suz12 was enriched on the Xi in a very small number of these female somatic cells (Figure 11B). Therefore, we conclude that Suz12 functions in maintenance of X-inactivation by a mechanism that, at most, requires only transient enrichment on the Xi.

In transformed mouse fibroblasts the DAPI-intense regions stained less intensely than the rest of the nucleus with Suz12 antibodies (Figure 11A, B), suggesting that endogenous Suz12 does not accumulate on constitutive heterochromatin. This contrasts a previous study, which reported that tagged over-expressed SUZ12 co-localized with tagged, over-expressed HP1a in COS-1 cells, a transformed monkey kidney cell line (Yamamoto *et al.*, 2004). These differing results may be due to differences in cell type or species or due to detection of endogenous versus over-expressed, tagged proteins.

Knockdown of SUZ12 in human somatic cells results in loss of H3-3mK27

Knockdown of SUZ12 in human somatic cells and a mutation of *Suz12* in mouse embryos cause a significant decrease in amounts of H3-3mK27, indicating that SUZ12 contributes to H3-K27 methylation (Cao and Zhang, 2004b; Kirmizis *et al.*, 2004; Pasini *et al.*, 2004). We undertook a single cell analysis to determine if SUZ12 is required for EED/EZH2 complex-mediated H3-K27 methylation on the Xi, employing female human fibroblast IMR90 cells, which were significantly more efficiently transfected with siRNAs than mouse embryo fibroblasts. Immunostaining was used to assay the abundance and distribution of H3-3mK27 in IMR90 cells transfected with siRNA oligonucleotides directed against SUZ12 or GFP RNA.

Untransfected and GFP siRNA transfected IMR90 cells exhibited abundant nuclear staining for H3-3mK27 (Figure 12A and data not shown). In 70% of interphase nuclei there was enrichment of this methylated form of H3 on the Xi, as visualized by co-localization with *XIST* RNA (Figure 12A). This result indicates that in IMR90 cells, Xi-enrichment of H3-3mK27 is maintained in a majority of cells, as previously reported for other somatic cell types (Gilbert *et al.*, 2003). The remaining 30% of GFP siRNA transfected cells showed a similar intensity of uniform nuclear H3-3mK27 staining, without enrichment on the *XIST* RNA-coated Xi (Figure 12B). GFP siRNA transfected IMR90 cells exhibited a uniform, speckled nuclear distribution of SUZ12 in 100% of cells with no apparent enrichment on the Xi, even in cells that showed Xi-accumulation of H3-3mK27 (Figure 12C, D).

Transfection of cells with SUZ12 siRNA resulted in complete knockdown in half of the cell population (Figure 12E, F). While a small proportion of cells lacking SUZ12 displayed normal H3-3mK27 staining either with or without Xi-enrichment (12% of cells; Figure 12F), the majority of cells with no detectable SUZ12 did not accumulate H3-3mK27 (88% of cells, Figure 12F). Cells lacking SUZ12 still retained an *XIST* RNA-coated Xi (Figure 12G), demonstrating that H3-3mK27 enrichment on the Xi is not required for *XIST* RNA to associate with the Xi in these cells. Knockdown of Suz12 in transformed mouse embryo fibroblasts also resulted in complete loss of detectable Suz12 and H3-3mK27 staining in a fraction of cells (data not shown). These datum indicate that complete knockdown of SUZ12 results in the global loss of H3-3mK27. Thus SUZ12 is necessary for enrichment of H3-3mK27 on the Xi in somatic cells, even though it is not detectably enriched there. This result also demonstrates that a local enrichment of

SUZ12 is not required for a local increase in H3-3mK27 histone methyltransferase activity during the maintenance phase of X-inactivation.

V. Discussion

Suz12 is enriched on the Xi during initiation of X-inactivation (de Napoles et al. 2004). Here we demonstrate that Suz12 Xi-enrichment is transient during early stages of X-inactivation in embryonic and extra-embryonic cells. While Suz12, Eed, and Ezh2 showed very similar patterns of enrichment on the Xi during development, the total amount of Suz12 remained fairly constant throughout differentiation while Ezh2 and Eed levels steadily decreased. Suz12 Xi-enrichment required *Xist* RNA, consistent with a role for *Xist* RNA in targeting Suz12 to the Xi as part of the Eed/Ezh2 complexes. Single cell analysis revealed that complete knockdown of SUZ12 resulted in loss of all detectable H3-3mK27 accumulation on the Xi and in other genomic regions, consistent with a role for SUZ12 in H3-K27 methylation of the Xi.

The developmentally regulated decrease in abundance of Eed and Ezh2 but not Suz12 suggests one of two possibilities: Suz12 may be a non-stochiometric component of the Eed/Ezh2 complexes in differentiated cells, or it may have functions outside its role as part of the Eed/Ezh2 complexes. Analysis of *in vitro* reconstituted EED/EZH2 complexes, as well as material purified from human somatic cells, indicates that SUZ12 is present in equimolar amounts with EED and EZH2 in active histone methyltransferase complexes, making it unlikely that Suz12 is required in excess *in vivo* (Cao *et al.*, 2002; Kuzmichev *et al.*, 2002; Kuzmichev *et al.*, 2004). Thus it seems likely that Suz12 may have activities that are independent of its role in the Eed/Ezh2 complexes.

Drosophila Su(z)12 is unique among PcG genes in that null and hypomorphic mutations are strong suppressors of position effect variegation, suggesting that in flies Su(z)12 has functions beyond PcG-mediated facultative heterochromatin formation. The majority of mutations that affect position effect variegation alter the activity of proteins involved in constitutive heterochromatin formation. In mammals and flies, facultative and constitutive heterochromatin are characterized by histone H3 methylation at different lysine residues, mediated by the Eed/Ezh2 and Suv39h histone methyltransferases (Jenuwein and Allis, 2001; Cao and Zhang, 2004a). Additionally, RNAs are implicated in directing these histone methyltransferases to their genomic targets in mammals and fission yeast (Hall *et al.*, 2002; Maison *et al.*, 2002; Volpe *et al.*, 2002; Plath *et al.*, 2003; Silva *et al.*, 2003; Volpe *et al.*, 2003). Therefore an additional role for Suz12, as suggested by its differential developmental regulation from other PcG proteins, may be to function in constitutive heterochromatin formation, perhaps by affecting activity or targeting of additional histone methyltransferase complexes.

VI. Figure Legends

Figure 5. Levels of Suz12 are similar in somatic cells and embryonic stem cells. (A) Western analysis of Ezh2, Suz12, Eed, and tubulin levels in transformed mouse fibroblast cells and ES cells. Levels of Ezh2, Suz12 and Eed are abundant in ES cells, whereas only Suz12 is detectable in fibroblast cells. (B, C) Immunostaining for Ezh2 (first column) and Eed (second column) in (B) undifferentiated ES cells and (C) a transformed mouse fibroblast cell line. DAPI delineates the nucleus (third column) and the merge (fourth column) is an overlay of Ezh2 (green) and Eed (red). (D, E) Immunostaining for Suz12 (first column) and Eed (second column) in (D) undifferentiated ES cells and (E) a transformed mouse fibroblasts cell line. DAPI delineates the nucleus (third column) and the merge (fourth column) is an overlay of Suz12 (green) and Eed (red).

Figure 6. Levels of Suz12 remain constant throughout stem cell differentiation. (A, B) Western analysis of Ezh2, Suz12, H3-3mK27, RbAp, and tubulin levels in differentiating ES (A) and TS (B) cells.

Figure 7. Suz12 is enriched on the Xi in differentiating ES cells during the onset of X-inactivation. (A, B) Immunostaining for Suz12 (first column) was combined with FISH for *Xist* RNA (second column) in undifferentiated (A) and differentiated (B) ES cells. DAPI delineates the nucleus (third column) and the merged image (fourth column) consists of Suz12 (red) and *Xist* RNA (green). (A) In undifferentiated ES cells, X-inactivation has not occurred and *Xist* is not expressed. Suz12 is diffuse throughout the nucleus. (B) In differentiated ES cells, *Xist* is expressed from the Xi and this is

accompanied by Xi-enrichment of Suz12. (C, D) Immunostaining for Suz12 (first column) and Eed (second column) in undifferentiated (C) and differentiated (D) ES cells. DAPI delineates the nucleus (third column) and the merged image (fourth column) is an overlay of Suz12 (red) and Eed (green). (C) Suz12 and Eed are diffusely distributed in undifferentiated ES cells. (D) Four days after induction of differentiation, Suz12 accumulates on the Xi, which is marked by Eed enrichment. (E) Graph indicating the percentage of ES cells with an *Xist* RNA-coated Xi accompanied by enrichment of Eed (gray bar) or Suz12 (black bar) during a differentiation time course (n>100).

Figure 8. Distribution of Suz12 in female blastocysts. (A, B) Immunostaining for Suz12 (first column) and Eed (second column) in cultured blastocysts. DAPI delineates the nuclei (third column) and the merged image (fourth column) consists of Suz12 (red) and Eed (green). (A) Female blastocysts cultured for 4 days. The Xi in differentiated extra-embryonic cells that have migrated away from the ICM, marked by the accumulation of Eed, is also enriched for Suz12 (arrow). (B) Xi-enrichment of Eed and Suz12 is lost in most extra-embryonic cells from blastocysts cultured for 8 days (arrow).

Figure 9. Differentiating trophoblast stem (TS) cells exhibit a transient enrichment of Suz12. (A-E) Immunostaining for Suz12 (green, first column) and H3-3mK27 (red, second column) in TS cells throughout several timepoints during differentiation. DAPI (third column) delineates the nuclei and the merged image (fourth column) consists of Suz12 and H3-3mK27. (A, B) At day 0 and day 2 of TS differentiation, Suz12 is

enriched on the Xi, as marked by H3-3mK27 . (C) Suz12 Xi-accumulation is lost completely by day 4. (E) Loss of the histone methylation mark is observed by day 8.

Figure 10. Xi-recruitment of Suz12 is dependent on *Xist*. (A) *Xist* RNA coating is sufficient to recruit Suz12. Immunostaining for Suz12 (first column) with FISH for *Xist* RNA (second column) in a male ES cell with a tet-inducible promoter upstream of the single *Xist* gene. DAPI (third column) demarcates the nucleus and the merged image (fourth column) is comprised of Suz12 (red) and *Xist* RNA (green). (A) Non-induced cells lack an *Xist* coated body and no enrichment of Suz12 is observed. (B) Induction of *Xist* expression results in coating of the single X chromosome and subsequent recruitment of Suz12.

Figure 11. Two patterns of Suz12 distribution in somatic cells. (A, B) Immunostaining for Suz12 (first column) with FISH for *Xist* RNA (second column) in mouse embryonic fibroblasts (MEFS), which are aneuploid and in some instances have more than one Xi. DAPI demarcates the nucleus and the merged image is comprised of Suz12 (red) and *Xist* RNA (green). (A) Staining pattern observed in a majority of cells. Suz12 is diffusely nuclear in somatic cells but do not exhibit an enrichment of Suz12 on the *Xist* RNA-coated Xi. (B) Staining pattern observed in a small proportion of cells (<1%, n=100). Suz12 shows co-localization with *Xist* RNA.

Figure 12. Distribution of SUZ12 and H3-3mK27 in SUZ12 knockdown cells. (A, B) FISH for *XIST* RNA (first column) was combined with immunostaining for H3-3mK27

(second column) in IMR90 primary human fibroblasts. DAPI delineates the nucleus (third column) and the merged image (fourth column) consists of *XIST* RNA (green) and H3-3mK27 (red). Cells exhibit two patterns of H3-3mK27 distribution, fairly uniform nuclear distribution of fine speckles with (A) or without enrichment on the Xi (B). (C-E) Immunostaining for SUZ12 (first column) and H3-3mK27 (second column) in IMR90 cells treated with GFP siRNAs (C, D) or SUZ12 siRNAs (E). Nuclei are stained with DAPI (third column) and the merged image (fourth column) consists of SUZ12 (red) and H3-3mK27 in green. (C, D) SUZ12 is distributed uniformly throughout the nucleus with many larger speckles of more intense staining in GFP siRNA treated cells, the same distribution that is observed in mock transfected or untransfected cells (data not shown). e After SUZ12 siRNA treatment, half the cells exhibited little or no SUZ12 staining. The majority of these cells contained no H3-3mK27. (F) FISH for *XIST* RNA (first column) was performed with immunostaining for H3-3mK27 (second column) in IMR90 cells subjected to SUZ12 siRNA. DAPI delineates the nucleus (third column) and the merged image (fourth column) consists of *XIST* RNA (green) and H3-3mK27 (red). *XIST* RNA still coats the Xi in cells lacking H3-3mK27. (G) Graph indicating the proportion of nuclei in GFP siRNA treated and SUZ12 siRNA treated cells with different patterns of H3-3mK27 distribution (n>100 cells). Only SUZ12 siRNA treated cells lacking SUZ12 were used for this analysis. Diagonal striped bars indicate proportion of cells with normal levels of H3-3mK27 and no enrichment on the Xi, grey bars indicate the proportion of cells with normal H3-3mK27 levels and Xi-enrichment, white bars indicate reduced nuclear staining with Xi-enrichment, and black bars indicate no detectable H3-3mK27 staining.

Figure 5

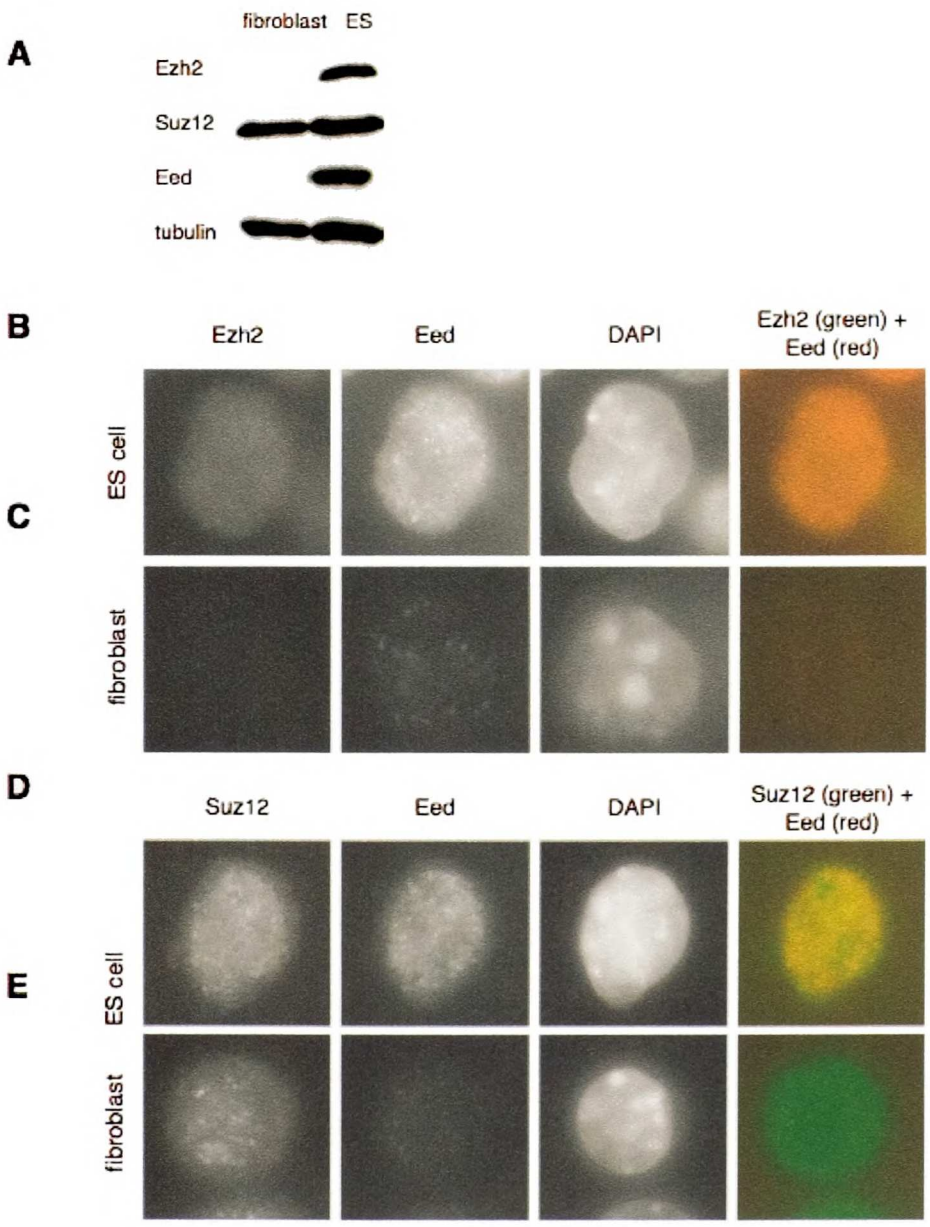
A
fibroblast
ES
Ezh2
Suz12
Eed
tubulin
B
Ezh2
Eed
DAPI
Ezh2 (green) +
Eed (red)
C
ES cell
fibroblast
D
Suz12
Eed
DAPI
Suz12 (green) +
Eed (red)
E
ES cell
fibroblast

Figure 6

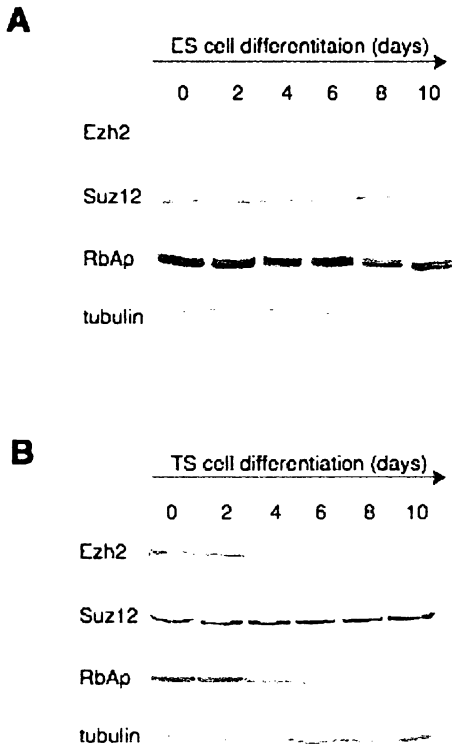
A
ES cell differentitaion (days)
0 2 4 6 8 10
Ezh2
Suz12
RbAp
tubulin
B
TS cell differentiation (days)
0 2 4 6 8 10
Ezh2
Suz12
RbAp
tubulin

Figure 7

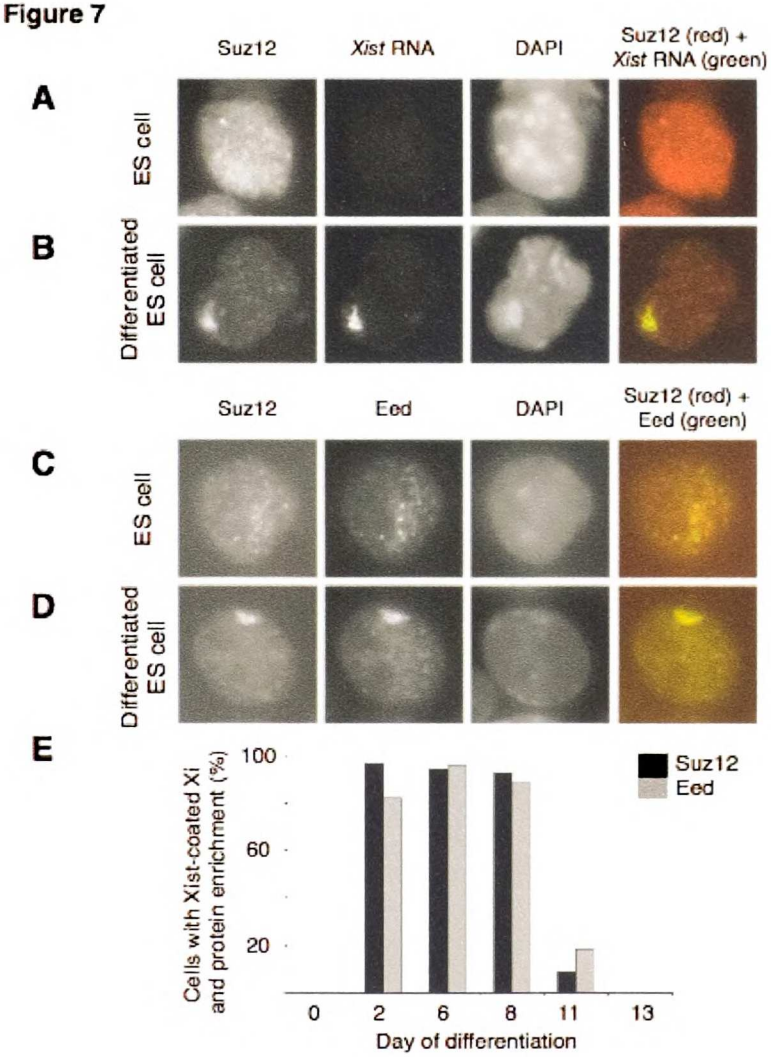
Suz12
Xist RNA
DAPI
Suz12 (red) + Xist RNA (green)
A
ES cell
B
Differentiated ES cell
Suz12
Eed
DAPI
Suz12 (red) + Eed (green)
C
ES cell
D
Differentiated ES cell
E
Cells with Xist-coated Xi and protein enrichment (%)
100
60
20
0
2
6
8
11
13
Day of differentiation
Suz12
Eed

Figure 8

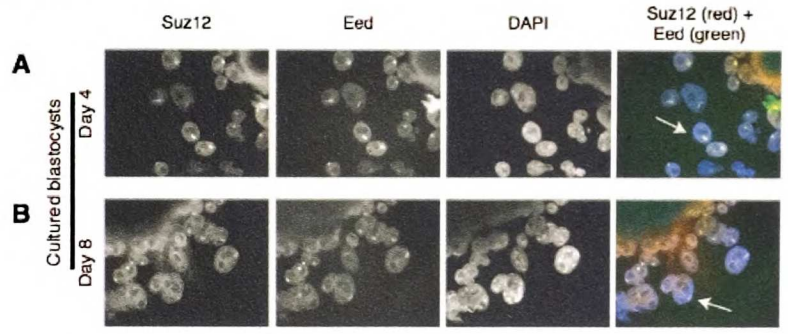
Suz12
Eed
DAPI
Suz12 (red) +
Eed (green)
A
B
Cultured blastocysts
Day 4
Day 8

Figure 9

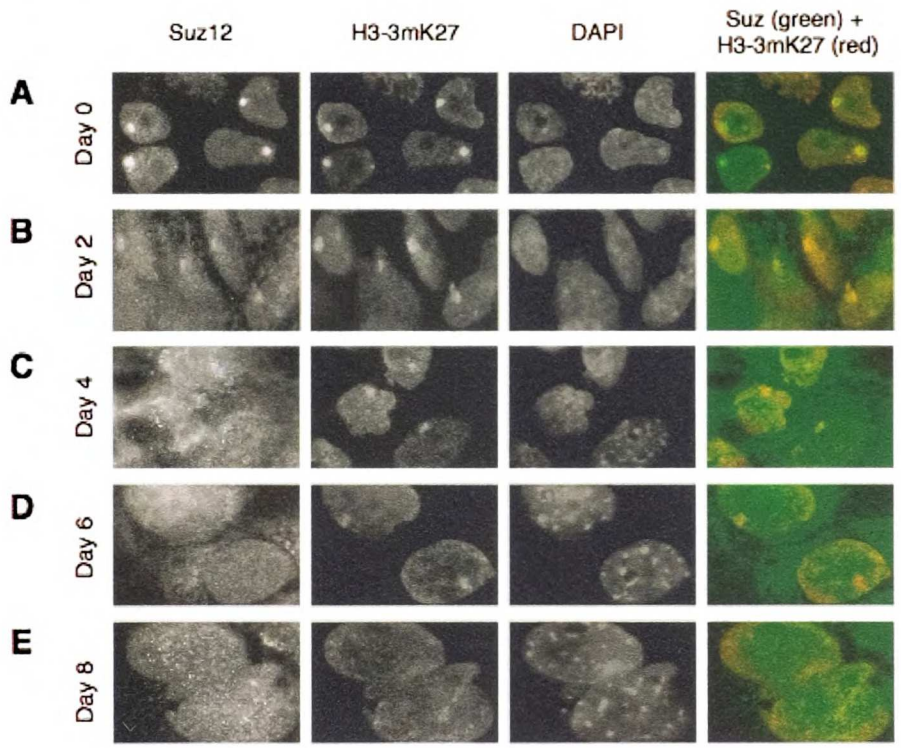
Suz12
H3-3mK27
DAPI
Suz (green) + H3-3mK27 (red)
A
Day 0
B
Day 2
C
Day 4
D
Day 6
E
Day 8

Figure 10

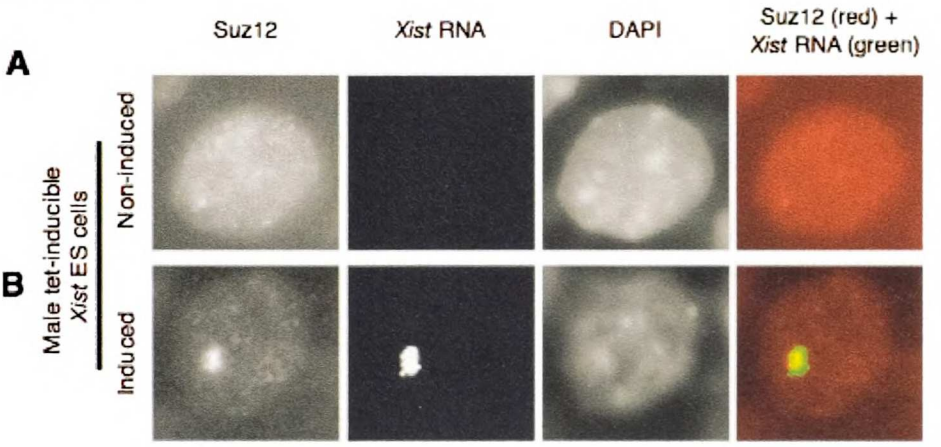
Suz12
Xist RNA
DAPI
Suz12 (red) +
Xist RNA (green)
A
B
Male tet-inducible
Xist ES cells
Non-induced
Induced

Figure 11

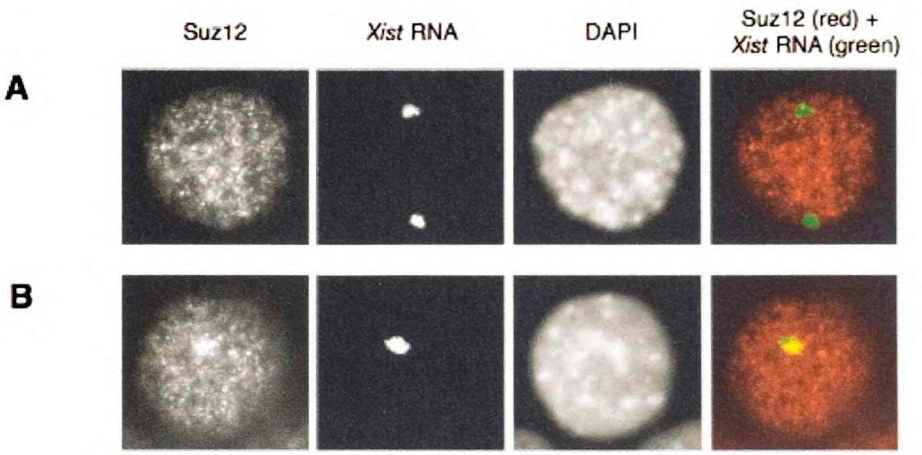

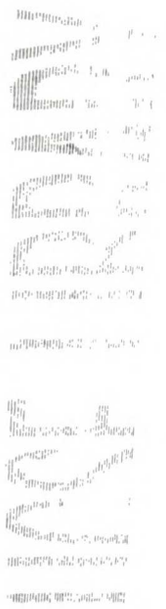

Figure 12

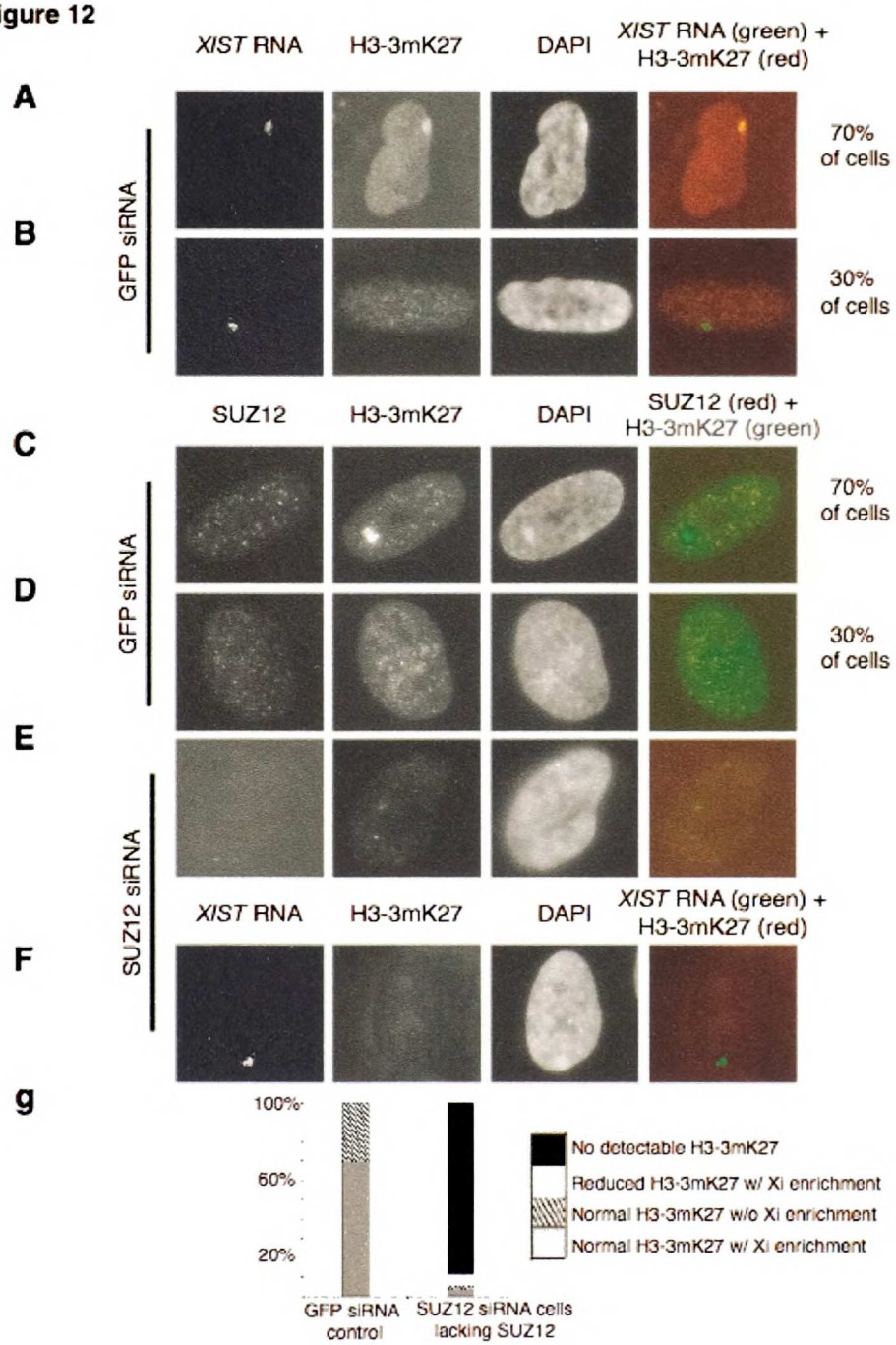
A
B
C
D
E
F
g
XIST RNA
H3-3mK27
DAPI
XIST RNA (green) + H3-3mK27 (red)
GFP siRNA
70% of cells
30% of cells
SUZ12
SUZ12 (red) + H3-3mK27 (green)
SUZ12 siRNA
100%
60%
20%
No detectable H3-3mK27
Reduced H3-3mK27 w/ Xi enrichment
Normal H3-3mK27 w/o Xi enrichment
Normal H3-3mK27 w/ Xi enrichment
GFP siRNA control
SUZ12 siRNA cells lacking SUZ12

CHAPTER 3

THE POLYCOMB GROUP PROTEIN SUZ12 REGULATES HISTONE H3 LYSINE 9 METHYLATION AND HP1α DISTRIBUTION

I. Abstract

Regulation of histone methylation is critical for proper gene expression and chromosome function. Suppressor of Zeste 12 (SUZ12) is a requisite member of the EED/EZH2 histone methyltransferase complexes, and is required for full activity of these complexes in vitro. In mammals and flies, SUZ12 /Su(z)12 is necessary for trimethylation of histone H3 on lysine 27 (H3-3mK27) on facultative heterochromatin. However, the phenotype of *Su(z)12* mutant flies suggested a function for Su(z)12 in constitutive heterochromatin formation. We investigated the molecular consequences of SUZ12 depletion in human cells. In addition to the expected loss of H3-3mK27, knockdown of SUZ12 also caused a reduction of bulk histone H3 lysine 9 tri-methylation (H3-3mK9) and altered the distribution of HP1α. In contrast, EZH2 knockdown caused loss of H3-3mK27 but not H3-3mK9, indicating that SUZ12 regulates H3-K9 methylation in an EZH2-independent fashion. This work uncovers a role for SUZ12 in H3-K9 methylation.

II. Introduction

Heterochromatin is the portion of the genome that is cytologically highly condensed. Different sequences are packaged into facultative heterochromatin in each cell type, allowing cells to stably maintain their unique expression patterns or cellular transcriptional memory. In contrast, constitutive heterochromatin is formed at pericentric and telomeric regions to epigenetically regulate centromere and telomere function in all cell types and developmental stages. Perturbation of heterochromatin can lead to aberrant gene expression and defective chromosome segregation, contributing to cancer and developmental disorders.

In *Drosophila*, the Polycomb Group (PcG) protein Suppressor of Zeste 12 (Su(z)12) is implicated in the formation of facultative and constitutive heterochromatin. PcG proteins assemble into several functionally and biochemically distinct complexes, termed Polycomb repressive complexes (PRCs), to mediate transcriptional silencing (Lehnertz *et al.*, 2003). PRC2-mediated silencing at *Drosophila Hox* loci requires methylation of histone H3 at lysine 27 (H3-K27) and/or lysine 9 (H3-K9) by the Enhancer of Zeste (E(z)) histone methyltransferase (HMTase) (Czermin *et al.*, 2002; Muller *et al.*, 2002; Breiling *et al.*, 2004). Suppressor of Zeste 12 (Su(z)12) is an essential component of the E(z) HMTase complex (Ketel *et al.*, 2005; Nekrasov *et al.*, 2005).

Genetic and biochemical analyses in *Drosophila* and *Schizosaccharomyces pombe* also implicate HMTases in the formation of constitutive heterochromatin. Suppressor of variegation 3-9 (Su(var)3-9) is an HMTase that methylates H3-K9 on constitutive heterochromatin (Rea *et al.*, 2000). Methylation of H3-K9 generates a binding site for the chromodomain of heterochromatin protein 1 (HP1) (Bannister *et al.*, 2001; Lachner *et al.*, 2001; Nakayama *et al.*, 2001). In addition, Su(var)3-9 and HP1 directly interact (Aagaard *et al.*, 1999; Melcher *et al.*, 2000; Grewal and Moazed, 2003; Yamamoto and Sonoda, 2003). It is postulated that propagation of constitutive heterochromatin occurs via a self-sustaining loop in which methylated H3-K9 binds HP1; HP1 in turn recruits more of the methyltransferase (Grewal and Moazed, 2003). *Drosophila* mutations in either *Su(var)3-9* or *Su(var)2-5*, the gene encoding HP1, exhibit defects in position effect variegation (PEV), the variable spread of silencing into euchromatic genes ectopically positioned in proximity to constitutive heterochromatin (Reuter and Wolff, 1981; Sinclair

et al., 1989). Su(z)12 is unique among PcG proteins because mutations of Suz12 exhibit strong defects in PEV, implicating this protein in regulation of constitutive heterochromatin (Birve *et al.*, 2001).

Mammals assemble constitutive and facultative heterochromatin structures by mechanisms that are homologous to those of *Drosophila.* The mouse homologues of *Su(var)3-9*, *Suvar39h1* and *Suvar39h2*, are required for the accumulation of tri-methylation of lysine 9 on histone H3 (H3-3mK9) and of the mammalian HP1 homologues, HP1α, HP1β and HP1γ, on pericentric heterochromatin (Bannister *et al.*, 2001; Lachner *et al.*, 2001; Nakayama *et al.*, 2001; Rice *et al.*, 2003). An HMTase complex that contains a murine homologue of E(z) is required for enrichment of H3-3mK27 on the facultative heterochromatin of the inactive X chromosome (Erhardt *et al.*, 2003; Plath *et al.*, 2003; Silva *et al.*, 2003). Human EZH2, in complex with different isoforms of another PcG protein EED, exhibits HMTase activity towards H3-K27, histone H1 lysine 26, and H3-K9 *in vitro* (Cao *et al.*, 2002; Kuzmichev *et al.*, 2002; Kuzmichev *et al.*, 2004). SUZ12, the human homologue of the fly PcG protein Suz(12), is a component of EED/EZH2 complexes and is necessary for the H3-3mK27 HMTase activity of the EED/EZH2 complex *in vivo* (Cao and Zhang, 2004b; Kirmizis *et al.*, 2004; Pasini *et al.*, 2004).

In addition to interacting with EZH2 and EED, SUZ12 also binds to HP1α (Cao and Zhang, 2004a; Yamamoto *et al.*, 2004), suggesting that, like the fly homologue, SUZ12 may play a role in constitutive heterochromatin formation in mammalian cells. Levels of murine Suz12 remain constant during mouse embryonic stem cell differentiation, while Eed and Ezh2 levels decrease, providing a second line of evidence

that Suz12 may function outside the Eed/Ezh2 complexes (de la Cruz *et al.*, 2005). To determine whether SUZ12 plays a role in constitutive heterochromatin formation, we examined levels and distribution of H3-3mK9 and HPα in cells that were depleted of SUZ12 by small interfering RNAs (siRNAs). Knockdown of SUZ12 resulted in a significant decrease of H3-3mK9 and in a redistribution of HP1α. SUZ12 knockdown also produced nuclear defects consistent with abnormalities in chromosome segregation, implicating SUZ12 in the regulation of pericentric heterochromatin formation and centromere function. In contrast, siRNA-mediated knockdown of EZH2, which reduced levels of H3-3mK27, did not alter the abundance or localization of H3-3mK9. These results suggest a role of SUZ12 in H3-K9 methylation that occurs in a manner independent of its interaction with EZH2.

III. Materials and Methods

Antibodies

The chicken H3-3mK9 antibody has been previously described (Plath *et al.*, 2003). Experiments using H3-3mK27 antibodies employed either a previously characterized chicken H3-3mK27 antibody (Plath *et al.*, 2003) or a mouse monoclonal antibody (ab6002, Abcam Inc.). Mouse monoclonal HP1α antibody (MAB3584) purchased from Chemicon was used for immunoflourescence and the mouse monoclonal HP1α antibody (07-346) purchased from Upstate was used for Western Blots. SUV39H1 antibody was obtained from Upstate (05615). Rabbit EZH2 and SUZ12 antibodies have been described previously (Cao *et al.*, 2002; Kirmizis *et al.*, 2004). The anti-histone H3 antibody (ab1791, Abcam Inc.), anti-actin antibody (sc-1615, Santa Cruz Biotechnology)

and anti-gamma tubulin antibody (GTU88, Sigma) was used for Western Blots. The H3-3mK9 antibody was used for Western blotting (ab8898, Abcam Inc.), A polyclonal GFP antibody (ab290, Abcam, Inc.) was used for immunoprecipitation experiments and Western Blots were performed with a monoclonal GFP antibody from BD Biosciences (JL-8). Monoclonal anti- c-Myc antibody was used for Western analysis and immunoprecipitation experiments (Santa Cruz Biotechnology, sc-40).

Cell culture

The IMR90 human female fibroblasts were purchased from American Type Culture Collection (ATCC, Cat # CCL-186) and cultured according to ATCC's handling procedures. HEK 293 cells were cultured in Dulbecco's modified Eagles' media with 10% fetal bovine serum and antibiotics.

siRNA transfection

SUZ12 siRNA SMARTpool (M0069570050), EZH2 siRNA SMARTpool (M00421800) and control GFP siRNA oligonucleotides (D0013000120) were obtained from Dhramacon Research Inc. siRNA duplexes were transfected into IMR90 cells using Lipofectamine 2000 (Invitrogen) according to manufacturer's instructions. Transfected cells were incubated with the siRNA for 72 hours, at which time they were harvested and re-plated at the original starting density. Cells were then re-transfected with the oligonucleotides and incubated for an additional 72 hours. After 6 days post-initial siRNA transfection the cells were harvested and processed for immunofluorescence and western blot analysis as detailed below.

Immunofluorescence (IF)

All cells were grown on coverslips. For Triton X-100 cytoskeleton extraction and IF of cells refer to Plath et al., 2003. The following secondary and tertiary antibodies were used for IF at a dilution of 1:200 (Vector Labs): Texas Red anti-mouse IgG, Texas Red anti-rabbit IgG, Fluorescein anti-mouse IgG. Cells that were not subjected to Triton X-100 extraction were fixed with 4% paraformaldehyde for 10 minutes, then directly incubated in blocking buffer as described in Plath et al., 2003.

Western blotting

IMR90 cells were harvested from the RNAi experiments and 5 x 10^5 cells from each treatment were boiled in 20 ul of loading dye (9% 2-mercaptoethanol, 9% SDS, 0.1% bromophenol blue, 30% glycerol) for 10 min. The denatured proteins were separated by SDS/PAGE on a 13% gel and transferred onto a nitrocellulose membrane. The membrane was incubated in blocking buffer (Tris-buffered saline with 0.1% Tween [TBS-T] and 5% nonfat dry milk) overnight at 4°C. The next day the membrane was incubated for 1 hr at room temperature with anti-SUZ12 antibody (Kirmizis *et al.*, 2004) anti-trimethyl H3-K27 antibody (ab6002, Abcam Inc.), anti-trimethyl H3-K9 antibody (ab8898, Abcam Inc.), anti-histone H3 antibody (ab1791, Abcam Inc.), or anti-actin antibody (sc-1615, Santa Cruz Biotechnology). After washing in TBS-T for 15 min, the blot was incubated for 1 hr with a horseradish peroxidase (HRP)-conjugated anti-rabbit secondary antibody (sc-2004, Santa Cruz Biotechnology) or an HRP-conjugated anti-mouse secondary antibody (sc-2005, Santa Cruz Biotechnology) and the signals were visualized by the enhanced chemiluminescence system as described by the manufacturer

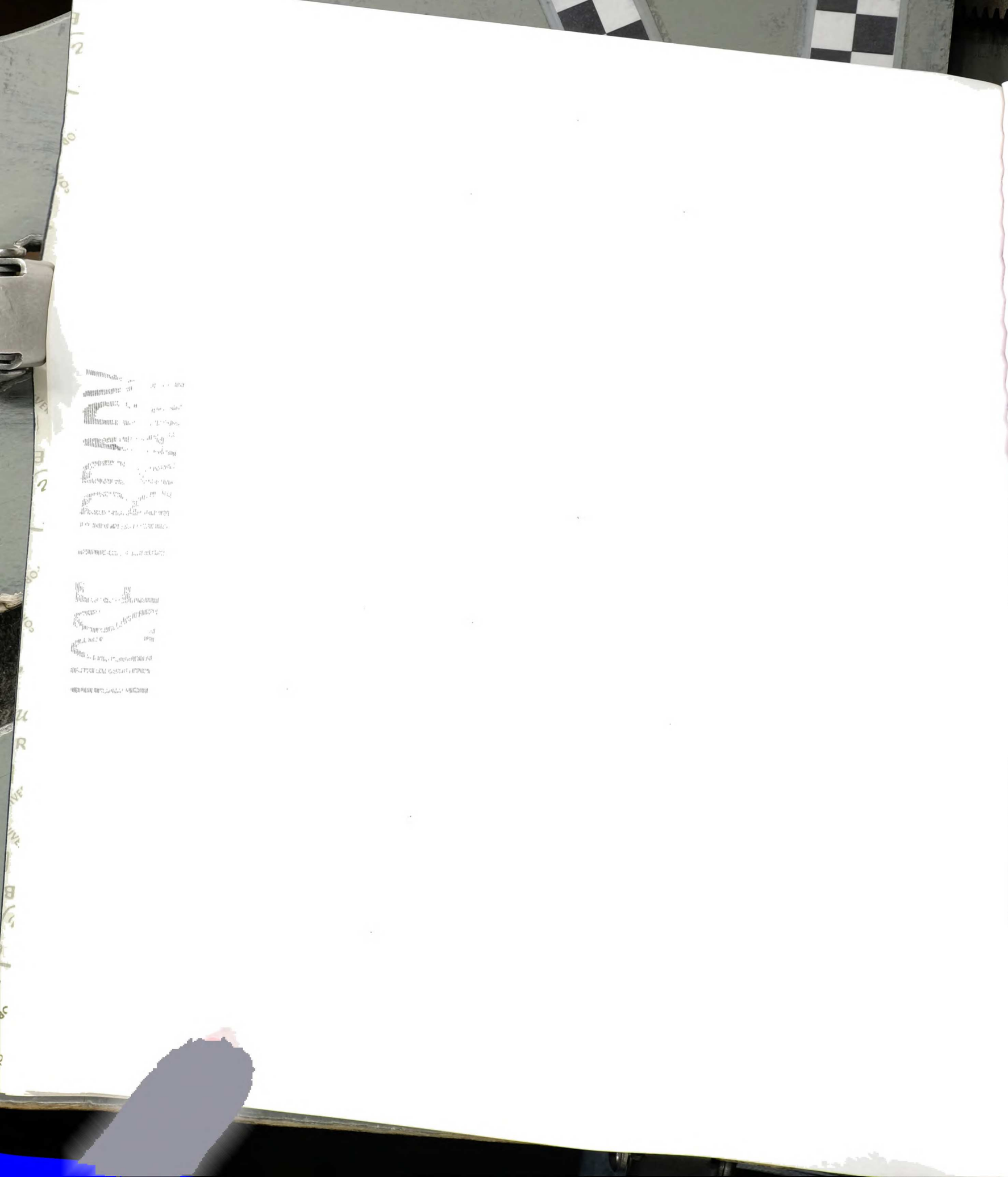

(RPN2106V, Amersham Biosciences). The H3-3mK9 and H3-3mK27 signals were quantified using ImageQuant and were normalized to the intensities of the histone H3 bands. Fold changes were calculated from the SUZ12 or EZH2 siRNA treated samples compared to the mock transfected and GFP siRNA transfected samples.

Image acquisition

Images were acquired using an Olympus BX60 microscope with an Olympus 100x UplanApo oil immersion lens with a numerical aperture of 1.35. A Hamamatsu ORCA-ER camera was used to capture the images, using Openlab 3.1.7 software. Images were globally adjusted for brightness and contrast, merged and pseudo-colored using Adobe Photoshop 7.

IV. Results

SUZ12 knockdown decreases histone H3-K9 tri-methylation

Previously, we demonstrated that Suz12 levels remain constant throughout murine embryonic stem cell differentiation, whereas Eed and Ezh2 levels steadily decline, indicating that Suz12 may regulate heterochromatin formation in differentiated cells in a PRC complex-independent manner (de la Cruz *et al.*, 2005). To determine whether SUZ12 affects constitutive heterochromatin structure in mammalian cells, we performed siRNA-mediated knockdown of SUZ12 in a primary female human fibroblast cell line (IMR90). We tested if SUZ12 regulated the levels and/or distribution of H3-3mK9, which is enriched on pericentric heterochromatin (Lachner *et al.*, 2001; Peters *et al.*, 2001; Peters *et al.*, 2003; Rice *et al.*, 2003). Immunostaining of IMR90 cells treated with

GFP siRNA showed that SUZ12 levels remained abundant and were identical to non-treated cells, indicating that siRNA treatment did not adversely affect the cells (Figure 1A, data not shown). H3-3mK9 distribution in these cells was diffusely nuclear, with foci of strong enrichment as well as many speckles (Figure 13A). siRNA-mediated knockdown of SUZ12 resulted in loss of SUZ12 in about 50% of the population (de la Cruz *et al.*, 2005). H3-3mK9 levels were markedly reduced in 92% of these cells (Figure 13B, n>100). Western blot analyses of knockdown cells showed a two- to three-fold decrease of H3-3mK9 when compared to mock transfected and GFP siRNA transfected cells (Figure 13C). We sought to determine if the SUZ12 knockdown phenotype was specific for tri-methylation of H3-K9. To this end, we co-immunostained control cells and SUZ12 siRNA-treated cells for a marker of SUZ12 knockdown, H3-3mK27, and for di-methylated H3-K9 (H3-2mK9). There was no discernable difference in the levels of H3-2mK9 between GFP siRNA and SUZ12 siRNA transfected cells as assayed by immunofluorescence (Figures 13D and E). These results indicate that SUZ12 regulates levels of H3-3mK9 but not H3-2mK9.

Knockdown of EZH2 results in loss of H3-3mK27 but not H3-3mK9

EZH2/EED complexes have H3-K9 HMTase activity in vitro (Kuzmichev *et al.*, 2002). To determine if the H3-3mK9 phenotype of SUZ12 knockdown cells was due to abrogation of EZH2/EED H3-K9 HMTase activity, we performed EZH2 knockdown experiments. EZH2 knockdown cells were stained using antibodies against H3-3mK27 and H3-3mK9 to examine levels and distribution of these chromatin marks. GFP siRNA transfected IMR90 cells exhibit a very low level of EZH2 present in dim speckles (Figure

14A). After 6 days of incubation with EZH2 siRNAs, 44% of cells exhibited a loss of EZH2 accompanied by a drastic reduction of H3-3mK27 (Figure 14B). Cells treated with EZH2 siRNA were co-immunostained for H3-3mK27 and H3-3mK9 (Figures 14C and D). In contrast to SUZ12 knockdown, loss of EZH2 caused a reduction of H3-3mK27 staining but did not affect levels of H3-3mK9 (Figures 14C and D). Western blot analysis of EZH2 knockdown cells corroborated the immunofluorescence results: levels of H3-3mK27 were reduced 3-fold in EZH2 knockdown cells as compared to mock and GFP siRNA transfected cells, whereas H3-3mK9 levels were reduced by only 0.2-fold (Figure 14E). We conclude that the H3-3mK9 phenotype observed in SUZ12 knockdown cells is not linked to the reduction in the overall amount of H3-3mK27. In addition, these experiments indicate that the SUZ12 siRNA H3-3mK9 phenotype is due to the loss of a SUZ12 function that is independent of SUZ12's role in the EZH2/EED HMTase complexes.

HP1a distribution is altered in SUZ12 knockdown cells

Given that HP1 localization is regulated by H3-K9 methylation (Bannister *et al.*, 2001; Peters *et al.*, 2001; Maison *et al.*, 2002; Rice *et al.*, 2003; Pal-Bhadra *et al.*, 2004; Yamamoto *et al.*, 2004), we reasoned that localization of HP1α may be affected in SUZ12 knockdown cells with lowered levels of H3-3mK9. In 80% of GFP siRNA transfected IMR90 cells, H3-3mK9 exhibited strong foci of enrichment that overlapped with toroidal HP1a staining (Figure 15A) indicative of constitutive heterochromatin (Minc *et al.*, 1999; Nielsen *et al.*, 2001). These cells also showed a large number of fine speckles of HP1a that did not overlap with H3-3mK9 (Figure 15A). The remaining 20%

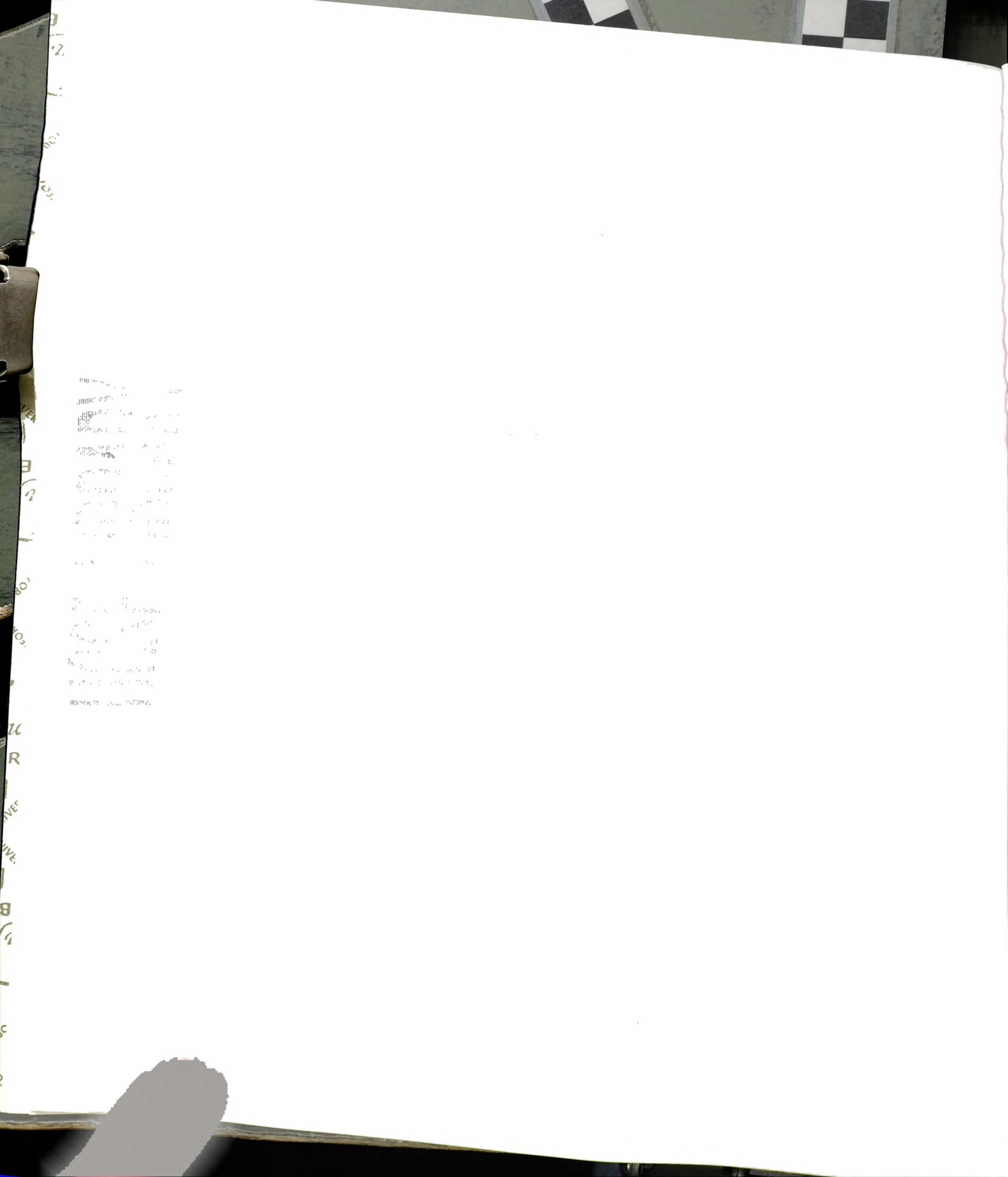

of GFP siRNA transfected cells displayed relatively uniform distribution of slightly larger HP1α speckles, and these cells always displayed a diffuse pattern of H3-3mK9 speckles, with no significant overlap between H3-3mK9 and HP1α (Figure 15B), consistent with dynamic localization of HP1α on constitutive heterochromatin (Cheutin *et al.*, 2003; Festenstein *et al.*, 2003; Hayakawa *et al.*, 2003). SUZ12 siRNA cells exhibiting low levels of H3-3mK9 displayed a diffuse pattern of HP1a in 87% of cells (n>100).

This diffuse distribution of HP1α in cells lacking H3-3mK9 staining was often accompanied by diminution in protein levels as detected by immunostaining (Figure 15C). HP1α is present in Triton X-100 soluble and insoluble pools, and the insoluble pools contain HP1α that is bound to heterochromatin (Taddei *et al.*, 2001). To test if SUZ12 knockdown affects total levels of HP1α or causes redistribution of HP1α from insoluble heterochromatin-associated pools to soluble, non-heterochromatin-associated pools, we performed immunostaining for H3-3mK9 and HP1α on SUZ12 knockdown cells that had (Figure 15C) or had not been Triton X-100 extracted prior to fixation (Figure 15D). Non- Triton extracted cells with lowered levels of H3-3mK9 contained diffusely distributed HP1α in amounts comparable to GFP siRNA treated cells (data not shown), but never had HP1α toroids. This result suggests that SUZ12 knockdown results in redistribution of HP1α from heterochromatin-associated pools to soluble pools. Immunostaining and Western blot analyses of H3-3mK27 (de la Cruz *et al.*, 2005) and H3-3mK9 (Figure 13) showed a decrease upon SUZ12 knockdown. In contrast, HP1α levels were not different between SUZ12 siRNA-treated cells and controls cells as assayed by Western blotting (Figure 15E). Because SUZ12 knockdown resulted in the

redistribution of HP1α from constitutive heterochromatin in a significant proportion of cells, we conclude that SUZ12 regulates the localization of HP1α.

Enrichment of HP1α on pericentric heterochromatin requires concomitant accumulation of H3-3mK9, and both of these marks are required for centromere function and normal chromosome segregation (Peters *et al.*, 2001; Taddei *et al.*, 2001). Given that levels of H3-3mK9 are reduced on pericentric heterochromatin in a significant fraction of SUZ12 knockdown cells, we expected that knockdown cells would exhibit defects in chromosome segregation. A common marker of chromosome instability is the appearance of micronuclei and chromatin bridges, which form when lagging chromosomes become surrounded by a nuclear envelope (Hoffelder *et al.*, 2004). Consistent with a defect in chromosome segregation, there was a 3-fold increase in the proportion of cells containing micronuclei and chromatin bridges in SUZ12 knockdown cells compared to the GFP siRNA treated cells (Figures 16A-C). These results suggest that centromere function is perturbed in SUZ12 knockdown cells.

SUV39H1 levels are not altered in SUZ12 knockdown cells

In mammalian somatic cells, SUV39H1 is the major HMTase that mediates tri-methylation of H3-K9. We performed Western blot analyses on mock transfected, GFP siRNA transfected, and SUZ12 siRNA transfected cells to determine if loss of this methyl mark in SUZ12 knockdown cells was due to a decrease in levels of SUV39H1. SUV39H1 was present in similar amounts in control and SUZ12 siRNA transfected cells, indicating that SUZ12 knockdown did not substantially alter the levels of SUV39H1 (Figure 17A). Immunostained GFP siRNA treated and SUZ12 knockdown cells was used to assay whether the distribution of SUV39H1 was affected in SUZ12 siRNA treated

cells. In GFP siRNA-treated cells, SUV39H1 was found in many speckles of variable intensity scattered throughout the nucleus (Figure 17B). We found that the levels and distribution of SUV39H1 were not detectably altered in cells lacking SUZ12, indicating that the altered levels of H3K9me3 detected in SUZ12 knockdown cells were not due to a loss or aberrant localization of the H3-K9 HMTase, SUV39H1 (Figure 17C).

V. Discussion

We have identified a role for the PcG protein SUZ12 in regulating levels of H3-3mK9 in primary human fibroblasts. Depletion of SUZ12 resulted in a loss of H3-3mK9, without affecting the abundance or distribution of the H3-3mK9 HMTase SUV39H1. We also observed a redistribution of HP1α upon SUZ12 depletion, consistent with the role of H3-3mK9 in the correct localization of HP1α (Lachner *et al.*, 2001; Peters *et al.*, 2001; Peters *et al.*, 2003; Rice *et al.*, 2003). Knockdown of SUZ12 lead to an increase in the proportion of cells with micronuclei and chromatin bridges, likely due to a defect in chromosome segregation due to perturbation of H3-3mK9/HP1α at constitutive heterochromatin (Peters *et al.*, 2001). In contrast, knockdown of EZH2 did not change the amounts of H3-3mK9, indicating that SUZ12 acts independently of EZH2 in regulation of H3-K9 tri-methylation. We conclude that SUZ12 acts outside of the EZH2/EED complexes to regulate the H3-3mK9/HP1α– containing heterochromatin. Together, these studies demonstrate that SUZ12 function is critical for correct formation of both constitutive heterochromatin and facultative heterochromatin.

In a recent study, knockdown of SUZ12 in HeLa cells had no discernible effect on H3K9me3 levels by Western blot (Cao and Zhang, 2004b), indicating that SUZ12 does not regulate H3-K9 tri-methylation in this transformed human cell type. The decrease in H3-3mK9 levels we observed in primary human fibroblasts could be due to differences in cell type, knockdown procedures, or method of analysis. In these fibroblasts, H3K9me3 levels were less sensitive than H3-3mK27 to SUZ12 knockdown, as a decrease in amounts of H3K27me3 could be detected after 3 days of siRNA treatment (data not shown), while the H3-3mK9 phenotype was only apparent after 6 days after siRNA treatment. This lag may be due to differences in stability of H3-3mK9 versus H3-3mK27. Our single cell analysis revealed that cells completely lacking SUZ12 exhibited dramatic depletion of H3-3mK9, an effect that was not apparent in analysis of cell populations by Western blotting.

Amounts and distribution of SUV39H1 were not detectably altered in SUZ12 knockdown cells, and a subset of SUV39H1 co-localized with SUZ12 in IMR90 cells, suggesting the possibility that SUZ12 may interact with SUV39H1 to regulate its activity. This suggests that SUZ12 may be present in different complexes: an EZH2/EED complex that mediates tri-methylation of H3-K27 on facultative heterochromatin, and a second complex that does not require EZH2 and regulates H3-3mK9 levels and HP1α distribution. HP1α enrichment on pericentric heterochromatin is no longer detected in mouse cells lacking the H3-3mK9 HMTases Suv39h1 and Suv39h2 (Lachner *et al.*, 2001; Peters *et al.*, 2001; Peters *et al.*, 2003; Rice *et al.*, 2003), suggesting that the redistribution of HP1α in SUZ12 knockdown cells may be an indirect effect of the decrease in H3-3mK9. The interaction between HP1 proteins and the SUV39H family of

HMTases plays a role in propagation of H3-K9 methylation (Grewal and Moazed, 2003). HP1α interacts with SUZ12 *in vitro* and myc-tagged SUZ12 and HA-tagged HP1α co-localize when transfected into HeLa cells (Yamamoto et al., 2004). This suggests an alternative possibility, that the decrease in H3-3mK9 staining observed in SUZ12 knockdown cells may occur indirectly, due to perturbation of SUZ12/HP1α complexes that are required for HP1α binding to H3-3mK9.

SUZ12 expression is mis-regulated in many human cancers, implicating SUZ12 in regulation of cell proliferation (Kirmizis et al., 2003). SUZ12 knockdown alters H3-K27 methylation and expression of SUZ12 target genes, such that changes in SUZ12 levels may perturb the expression of genes essential for normal growth and proliferation (Kirmizis et al., 2003). A high proportion of SUZ12 knockdown cells exhibit micronuclei and chromatin bridges, which correlate with aneuploidy (Jallepalli and Lengauer, 2001), suggesting that defects in SUZ12 –dependent chromatin may also contribute to tumorigenesis by increasing genomic instability. Our study demonstrates that the dual functions of SUZ12 in regulating both facultative and constitutive heterochromatin may be essential for maintaining appropriate gene expression as well as genomic integrity.

VI. Figure Legends

Figure 13. Distribution of H3-3mK9 and H3-2mK9 in SUZ12 knockdown cells. (A and B) Immunolocalization of SUZ12 (first column) and H3-3mK9 (second column) in IMR90 cells treated with GFP siRNA (A) or SUZ12 siRNA (B). Nuclei are stained with DAPI (third column) and the merged image (fourth column) consists of SUZ12 (red) and H3-3mK9 (green). (C) Western analysis of SUZ12, H3-3mK27, H3-3mK9, histone H3 and actin levels in mock, SUZ12 siRNA, and GFP siRNA transfected IMR90 cells. (D and E) Immunostaining for H3-3mK27 (first column) and H3-2mK9 (second column) in IMR90 cells treated with GFP siRNAs (D) or SUZ12 siRNAs (E). Nuclei are stained with DAPI (third column) and the merged panel (fourth column) consists of H3-3mK27 (green) and H3-2mK9 (red).

Figure 14. EZH2 knockdown results in depletion of H3-3mK27 but not H3-3mK9. (A and B) Immunostaining for EZH2 (first column) and H3-3mK27 (second column) in IMR90 cells treated with GFP siRNAs (A) or EZH2 siRNAs (B). Nuclei are stained with DAPI (third column) and the merged panel (fourth column) consists of EZH2 (red) and H3-3mK27 (green). (C and D) Immunostaining for H3-3mK27 (first column) and H3-3mK9 (second column) in IMR90 cells treated with GFP siRNAs (C) or EZH2 siRNAs (D). Nuclei are stained with DAPI (third column) and the merged panel (fourth column) consists of H3-3mK27 (red) and H3-3mK9 (green). (E) Western blotting for EZH2, H3-3mK27, H3-3mK9, and gamma tubulin in IMR90 cells transfected with no siRNA, SUZ12 siRNA, or GFP siRNA.

Figure 15. Distribution of HP1α in SUZ12 knockdown cells. (A and B) Immunolocalization of HP1α (first column) and H3-3mK9 (second column) in GFP siRNA treated IMR90 cells. Nuclei are stained with DAPI (third column) and the merged image (fourth column) consists of HP1α (red) and H3-3mK9 (green). HP1α and H3-3mK9 show two patterns of distribution: HP1α is present in many speckles, which in some instances are organized into toroids that overlap with H3-3mK9 toroids (A), and HP1α and H3-3mK9 show many speckles with no toroids and no significant amount of overlap (B). (C and D) Immunolocalization of HP1α (first column) and H3-3mK9 (second column) in SUZ12 siRNA treated IMR90 cells. In SUZ12 siRNA-treated cells that show little or no detectable H3-3mK9, HP1α is also not detectable when cells are extracted with Triton X-100 (C), but remains detectable in cells that were not Triton X-100 extracted (D). (E) Western blotting for SUZ12, HP1α, and histone H3 in IMR90 cells transfected with no siRNA, SUZ12 siRNA, or GFP siRNA.

Figure 16. Increase in micronuclei and chromatin bridges in SUZ12 knockdown cells. (A-C) Immunostaining for SUZ12 (second column) in IMR90 cells treated with GFP siRNAs (A) or SUZ12 siRNAs (B and C) Nuclei are stained with DAPI (first column) and the merged panel (third column) consists of SUZ12 (red) and DAPI (blue). (B) A SUZ12 knockdown cell with micronuclei. (C) A SUZ12 knockdown cell exhibiting a chromatin bridge.

Figure 17. Distribution of SUZ12 and SUV39H1 in SUZ12 knockdown cells. (A) Western blotting for SUZ12, SUV39H1, and gamma tubulin IMR90 cells transfected

with no siRNA, SUZ12 siRNA, or GFP siRNA. (B and C) Immunostaining for SUZ12 (first column) and SUV39H1 (second column) in IMR90 cells treated with GFP siRNAs (B) or SUZ12 siRNAs (C). Nuclei are stained with DAPI (third column) and the merged panel (fourth column) consists of SUZ12 (red) and SUV39H1 (green).

Figure 13

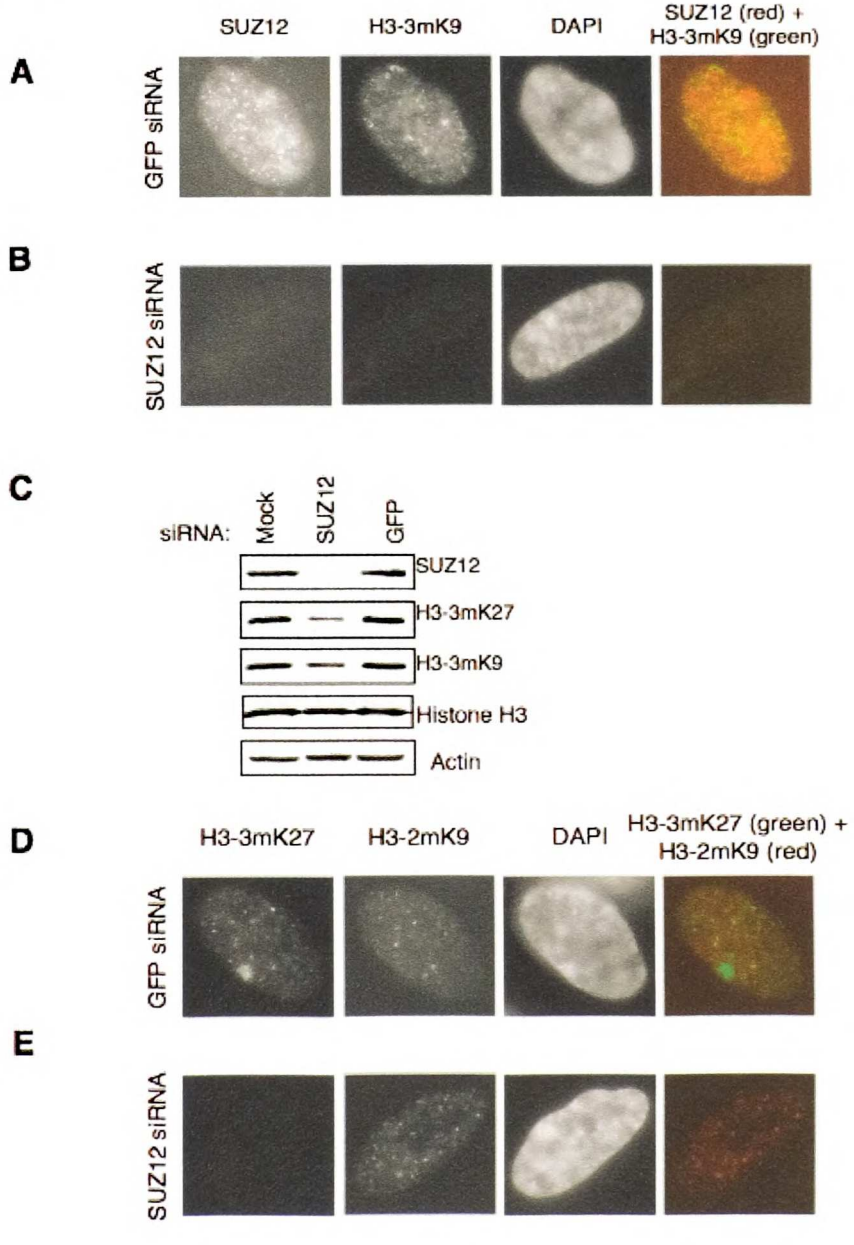
A
SUZ12
H3-3mK9
DAPI
SUZ12 (red) +
H3-3mK9 (green)
GFP siRNA
B
SUZ12 siRNA
C
siRNA:
Mock
SUZ12
GFP
SUZ12
H3-3mK27
H3-3mK9
Histone H3
Actin
D
H3-3mK27
H3-2mK9
DAPI
H3-3mK27 (green) +
H3-2mK9 (red)
GFP siRNA
E
SUZ12 siRNA

Figure 14

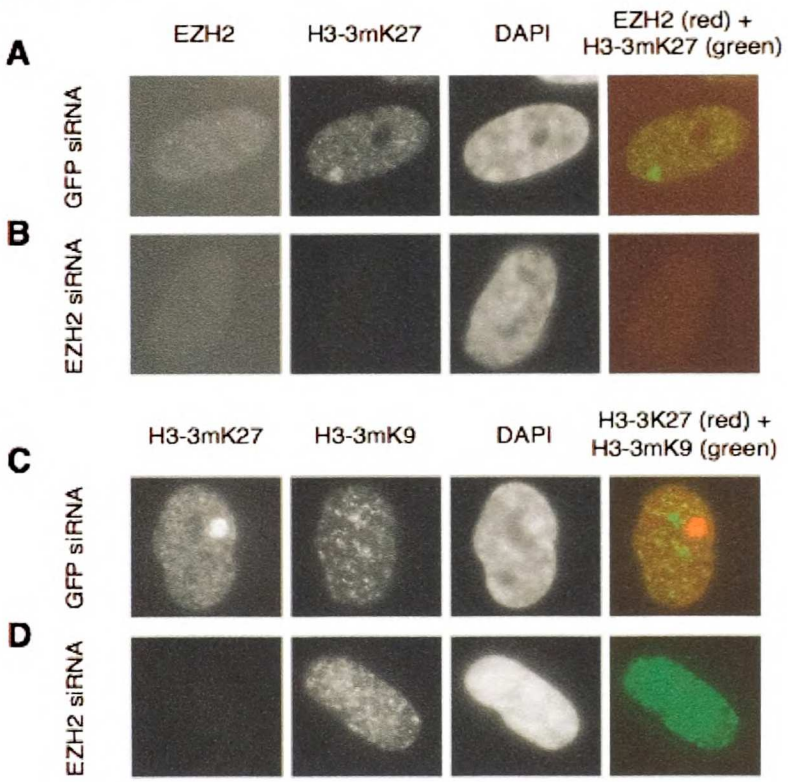
A
EZH2
H3-3mK27
DAPI
EZH2 (red) +
H3-3mK27 (green)
GFP siRNA
B
EZH2 siRNA
C
H3-3mK27
H3-3mK9
DAPI
H3-3K27 (red) +
H3-3mK9 (green)
GFP siRNA
D
EZH2 siRNA

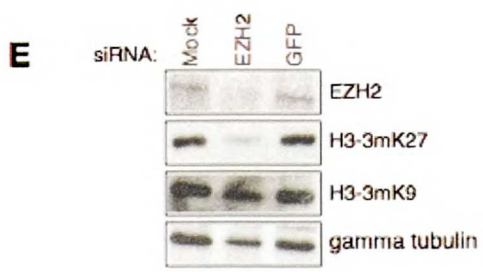
E
siRNA:
Mock
EZH2
GFP
EZH2
H3-3mK27
H3-3mK9
gamma tubulin

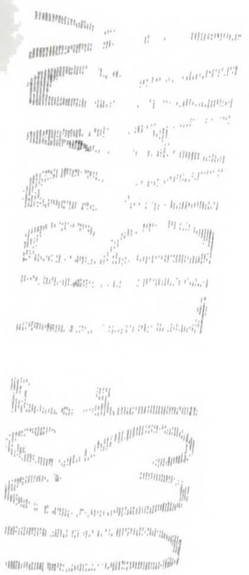

Figure 15

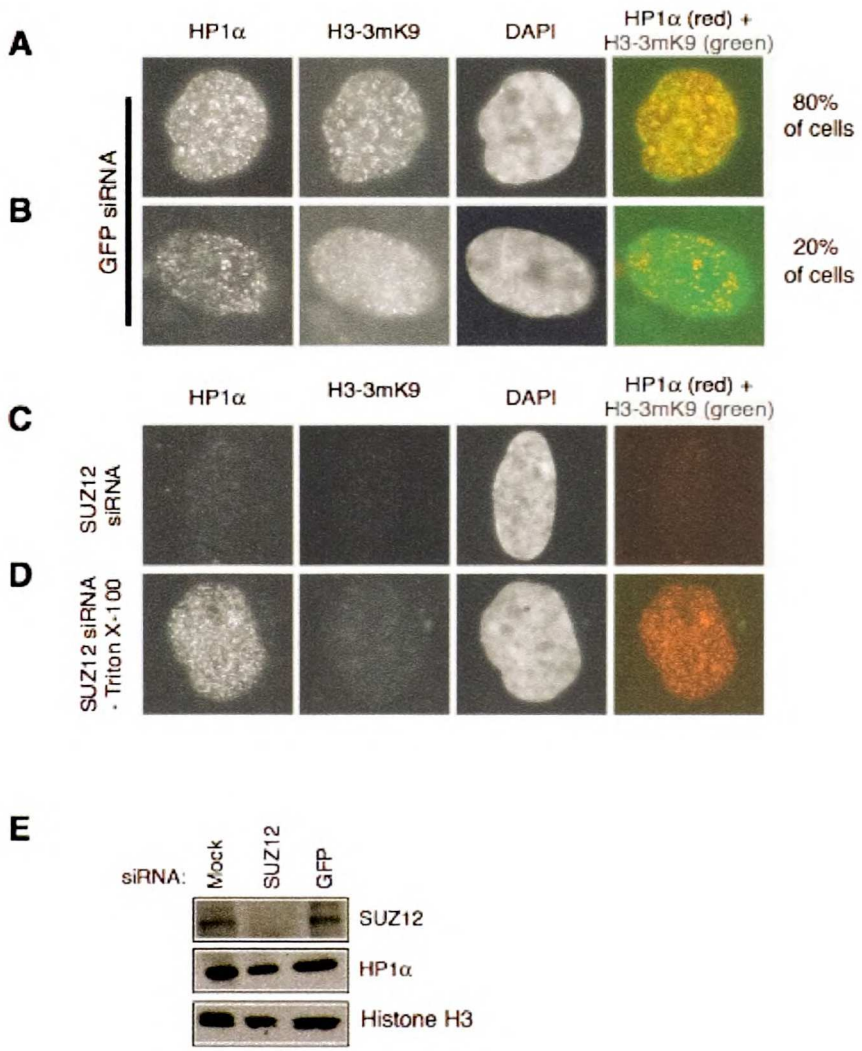
A
B
C
D
E
HP1α
H3-3mK9
DAPI
HP1α (red) +
H3-3mK9 (green)
GFP siRNA
80%
of cells
20%
of cells
SUZ12
siRNA
SUZ12 siRNA
- Triton X-100
siRNA:
Mock
SUZ12
GFP
SUZ12
HP1α
Histone H3

Figure 16

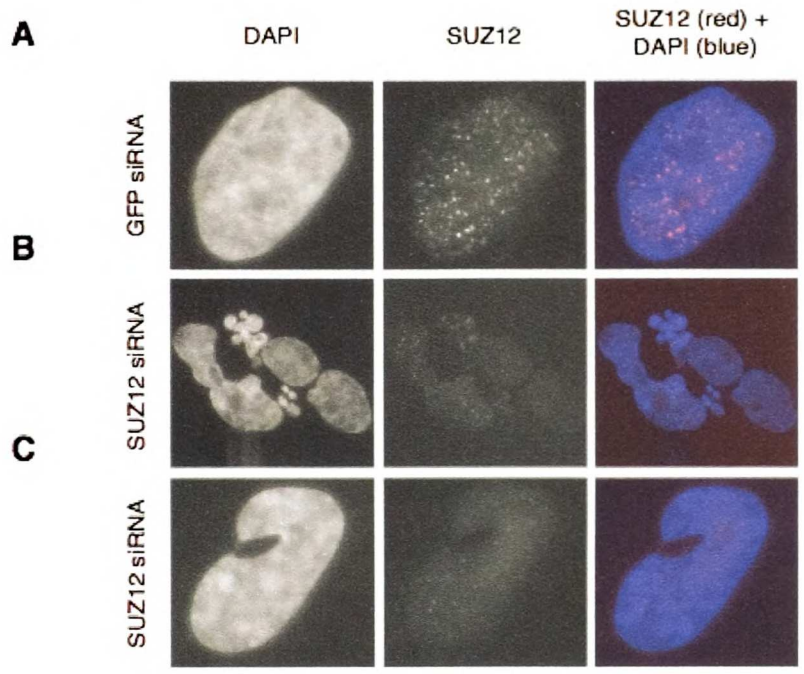
A
B
C
DAPI
SUZ12
SUZ12 (red) +
DAPI (blue)
GFP siRNA
SUZ12 siRNA
SUZ12 siRNA

Figure 17

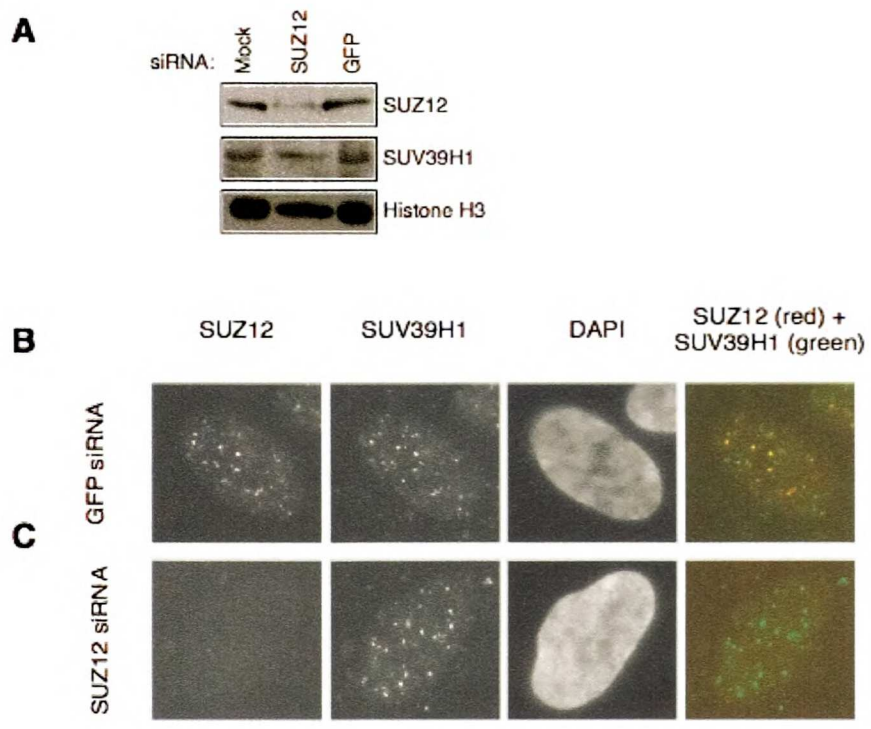
A
siRNA:
Mock
SUZ12
GFP
SUZ12
SUV39H1
Histone H3
B
SUZ12
SUV39H1
DAPI
SUZ12 (red) +
SUV39H1 (green)
C
GFP siRNA
SUZ12 siRNA

CONCLUDING REMARKS

X-inactivation in the developing mouse embryo

The X-inactivation developmental cue theory postulates that a differentiation-induced cue signals the onset of *Xist* expression and X-inactivation in the developing female embryo. In order to determine if X-inactivation *in vivo* occurs simultaneously with a defined developmental transition, I performed *in situ* hybridization studies for *Xist* RNA in female embryos. In the work described in chapter 1, I demonstrated that upregulation of of *Xist* expression occurs during the developmentally regulated process of cavitation at the age of 5.5dpc. Previously it was thought that *in vivo* random X-inactivation occurs as it does during *in vivo* imprinted X-inactivation and *in vitro* random X-inactivation: during the differentiation of a cell from a pluripotent to a somatic state.

The embryonic ectoderm does undergo a restriction in its multi-potency during the process of cavitation. Gardner and Rossant (Gardner and Rossant, 1979) demonstrated that the embryonic ectoderm loses the potential to form primitive endoderm cells by 5.0dpc. In addition, the cells of the 5.5dpc embryonic ectoderm are unable to contribute to the development of an embryo when implanted into host blastocysts (Gardner and Lyon, 1971; Brook and Gardner, 1997). Furthermore, the cells of the embryonic ectoderm at 5.5dpc are distinguished from the pre-cavitation embryo by differential expression of *Fgf5, Rex1*, and *Gbx2* (Haub and Goldfarb, 1991; Rogers *et al.*, 1991; Chapman *et al.*, 1997). Therefore while *in vivo* random X-inactivation does not occur concomitantly with a differentiation event, it does indeed correspond with a restriction of embryonic ectodermal cell fate.

I attempted *in vitro* cavitation and X-inactivation studies using cavitating EBs. Paraffin sectioning and FISH on EBs proved to be difficult, however. An alternative may be found in Early Primitive Ectoderm- Like (EPL) cells. By culturing ES cells in a defined, conditioned medium Rathjen and colleagues differentiated ES cells into the cell equivalent of the post-cavitated embryonic ectoderm (Rathjen *et al.*, 1999). If it can be shown that female EPL cells undergo X-inactivation in response to being cultured in the conditioned medium, then manipulation of EPL cells may serve as a useful *in vitro* system for studying the process of X-inactivation.

The silencing process of X-inactivation *in vitro* occurs in a series of three distinct events: initiation, establishment, and maintenance (Wutz *et al.*, 2002). During the initiation and establishment phases, continued *Xist* expression is required for transcriptional silencing of the X chromosome. The last step, the maintenance phase, is defined by the irreversible and *Xist*-independent continuance of X chromosome silencing. My studies, taken together with the work of the Rathjen lab, suggest that the developmental events that occur during cavitation may correlate with these three phases of X-inactivation. Through their studies with EPL cells, Rathjen and colleagues argue that formation of the fate-restricted embryonic ectoderm is an obligatory step in the differentiation of the inner cell mass or ES cells into the germ cell layers (Rathjen *et al.*, 1999). The timing of this transitional step, which occurs during the process of cavitation in the embryo, closely resembles the timing of the three phases of X-inactivation (Figure 18). Future studies could include investigation of whether the three phases of X-inactivation occur during the cavitation and gastrulation processes of the embryo.

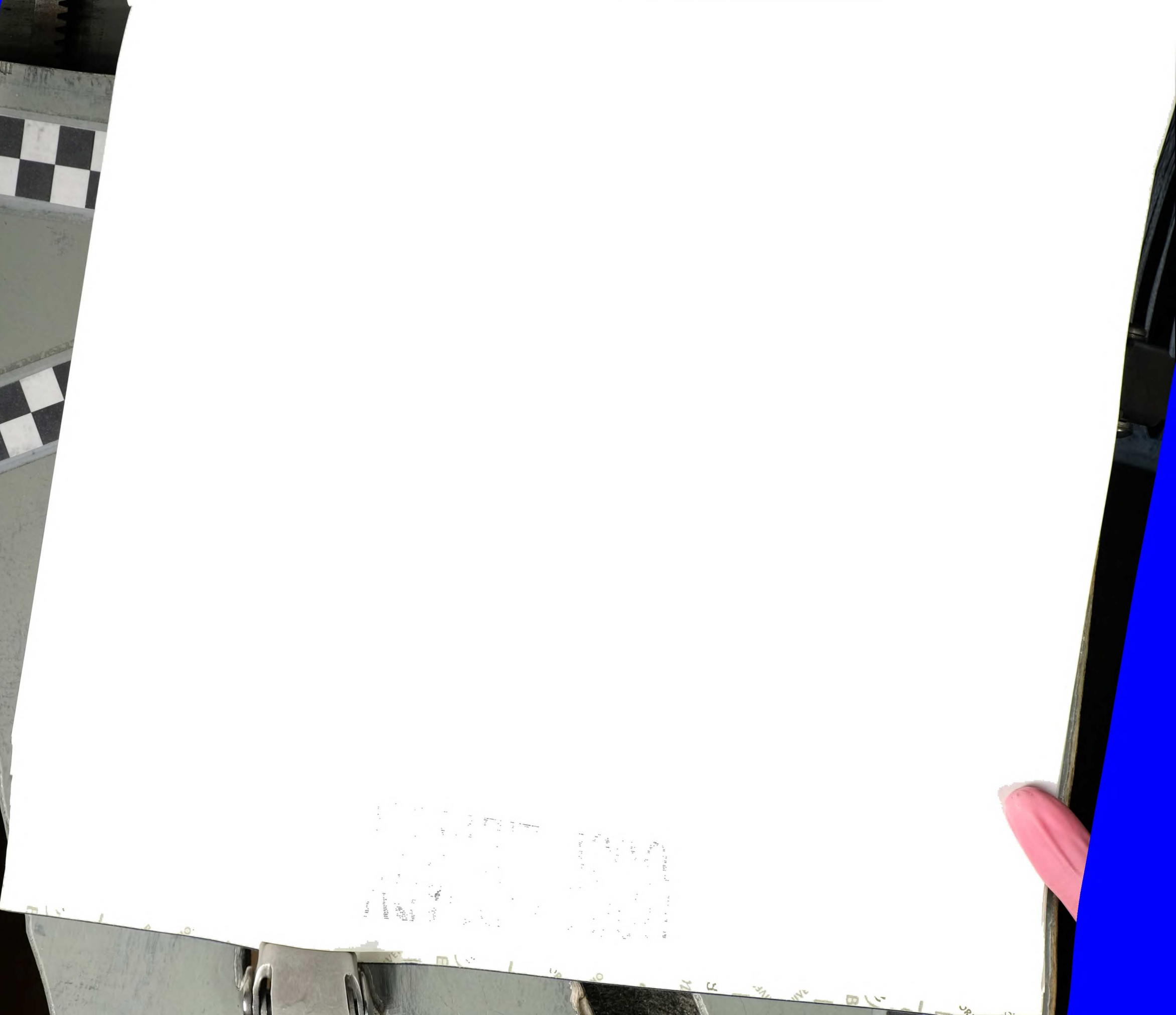

Another line of study that can be pursued using the techniques outlined in chapter 1 may be to determine the order of appearance or exclusion of chromatin modifications on the inactive X chromosome. Temporal studies of histone modifications on the Xi have been performed in ES cells as well as during imprinted X-inactivation of the early (two cell stage to 4.0dpc) embryo (Cohen *et al.*, 2005). These studies have already shown that significant differences exist between these two types of X-inactivation. It is therefore likely that random *in vivo* X-inactivation will differ from both random *in vitro* X-inactivation and imprinted *in vivo* X-inactivation. Performing IF for chromatin modifications in conjunction with FISH for *Xist* in post-cavitation embryos will thus provide the most biologically relevant analysis of how the facultative heterochromatin of the X chromosome is established. Such studies would determine whether X-inactivation *in vitro* truly mimics the events of X-inactivation *in vivo*.

Possible molecular roles for SUZ12 in H3-K9 tri-methylation

SUZ12 is a requisite member of the EED/EZH2 Polycomb Group Complex. Our group and others had shown that Eed and Ezh2 are involved in depositing the H3-3mK27 mark on the Xi during the initiation of X-inactivation. The work described in chapter 2 demonstrates that Suz12 is also transiently enriched on the Xi during X-inactivation and that it is required for enrichment of H3-3mK27 on the Xi. Differential protein expression of Suz12 with respect to Eed and Ezh2 suggested that Suz12 may have another role distinct from its function in H3-K27 tri-methylation. Chapter 3 contains data demonstrating that SUZ12 is required for H3-3mK9 in primary human fibroblasts. In addition, *in vitro* studies demonstrate that SUZ12 associates with SUV39H1 (Appendix),

suggesting that SUZ12 may exert its effect on constitutive heterochromatin through its interaction with the H3-3mK9 HMTase, SUV39H1.

Clues for the possible molecular functions of SUZ12 in the SUV39H1 methylation system may be found by considering its role in the Polycomb Repressive Complex. Studies of the *Drosophila* Esc/E(z) complex demonstrates that at least one role of Su(z)12 is to mediate binding of the complex to nucleosomes (Nekrasov *et al.*, 2005). Other studies suggest that Su(z)12 can potentiate activity of the HMTase E(z) (Ketel *et al.*, 2005). Taken together, Su(z)12 may regulate complex activity by directly contacting E(z) and by facilitating recruitment of the complex to its substrate. SUZ12 may be playing a similar role in regulating SUV39H1 activity.

Several lines of experimentation could determine if SUZ12 acts in the same way with SUV39H1 as it does with EZH2. One could perform ChIP/chip experiments for SUV39H1 in cells lacking SUZ12. If SUZ12 is required to bring SUV39H1 to the appropriate loci, one would expect that SUV39H1 distribution would be perturbed in cells lacking SUZ12. To determine if SUZ12 controls SUV39H1 HMTase function one could isolate SUV39H1 from cell extracts lacking SUZ12. The resulting SUV39H1 immunocomplexes could then be applied to an HMTase assay. If SUZ12 is required for proper enzymatic activity of SUV39H1 HMTase activity, then it would be expected that immunoprecipitates lacking SUZ12 would not behave as well as wild-type immunoprecipitates. Such studies would help to elucidate the molecular role of SUZ12 in H3-3K9 methylation and constitutive heterochromatin formation.

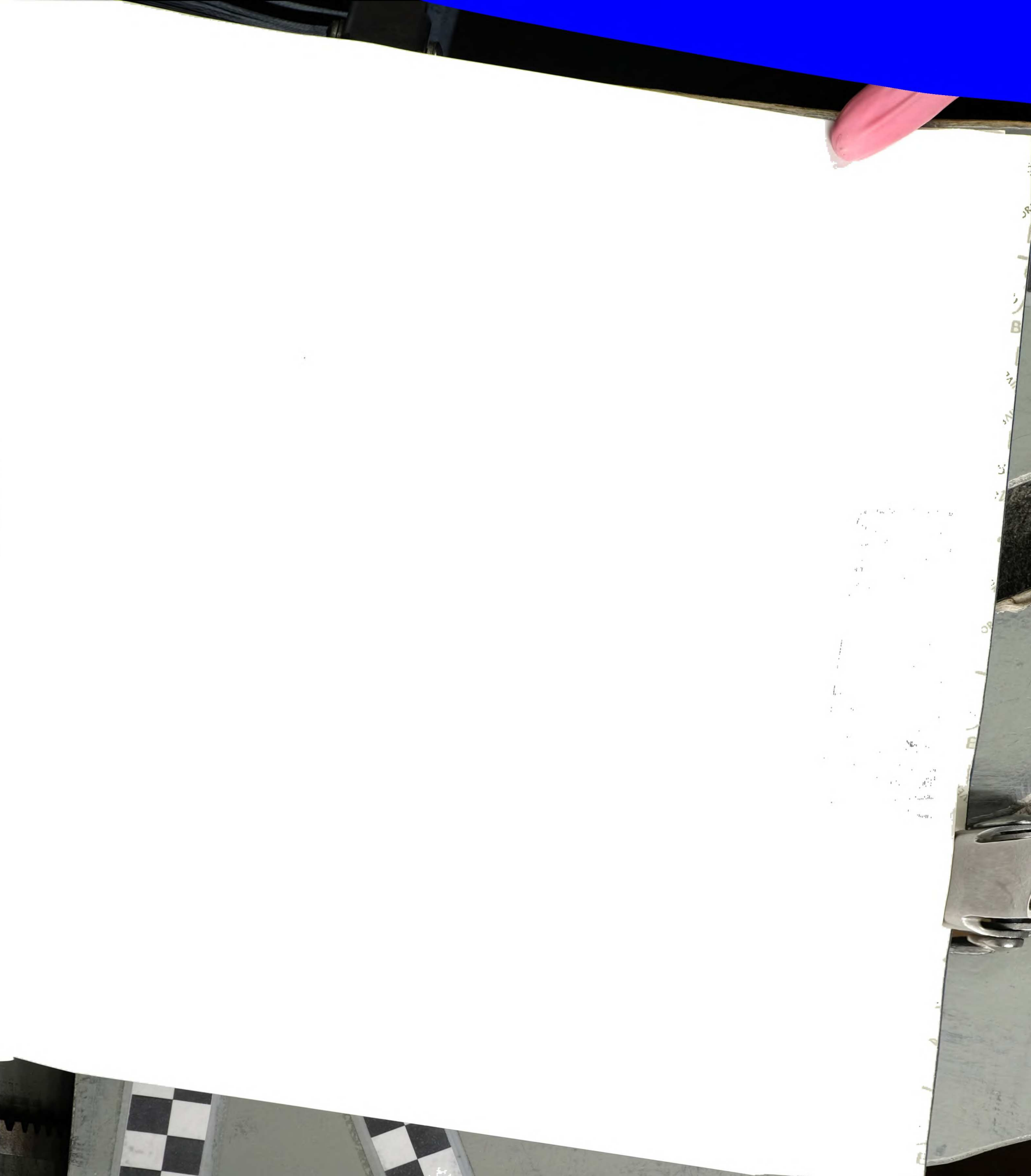

Figure Legends

Figure 18. The phases of X-inactivation temporally correlate with ES cell differentiation and embryonic development. The three phases of X-inactivation (Initiation, Establishment, Maintenance) occur on a time-scale similar to the three stages of ES cell differentiation (ES, Embryonic Primitive Ectoderm-Like (EPL), Differentiated), and development of the embryo proper.

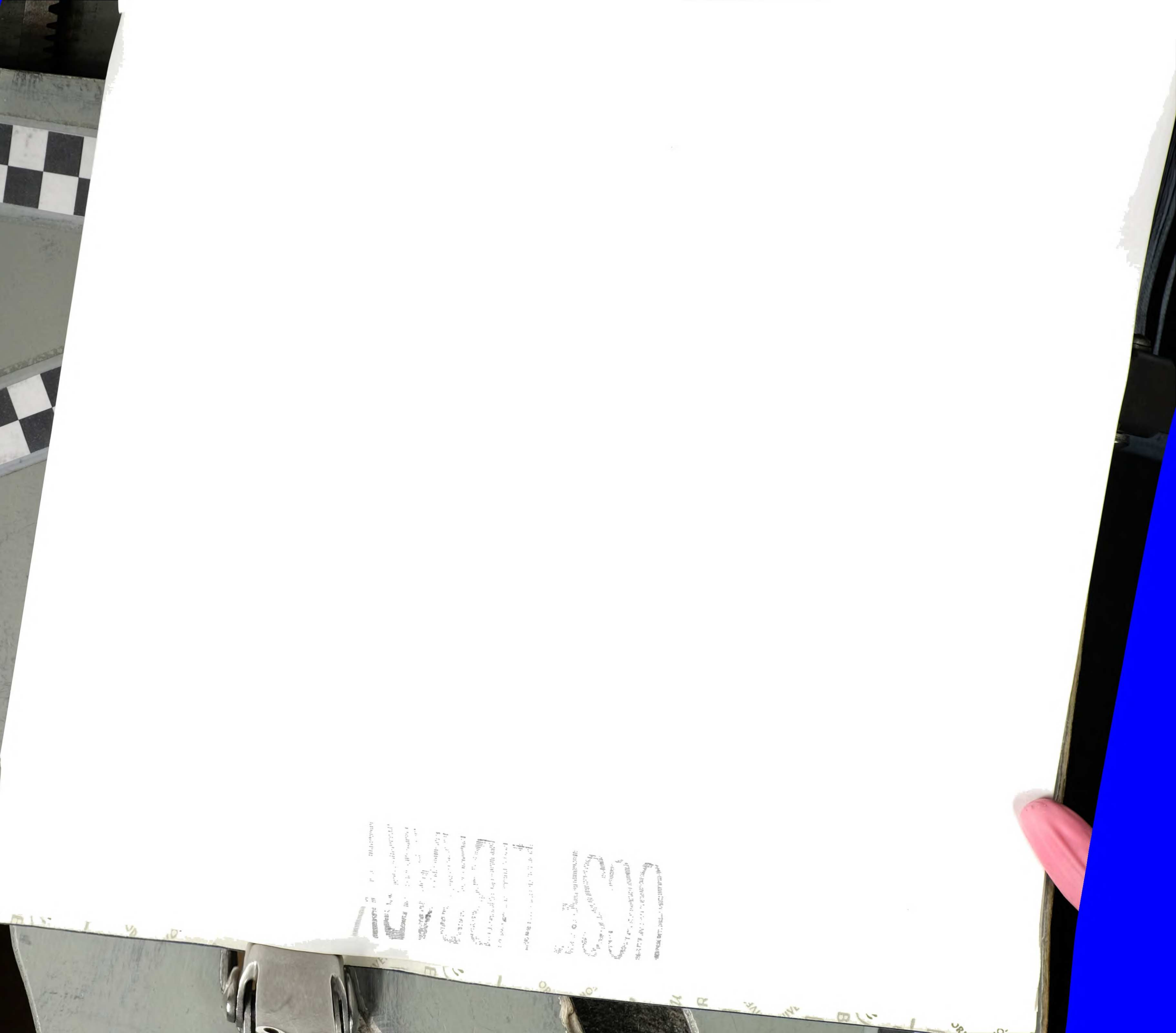

Figure 18

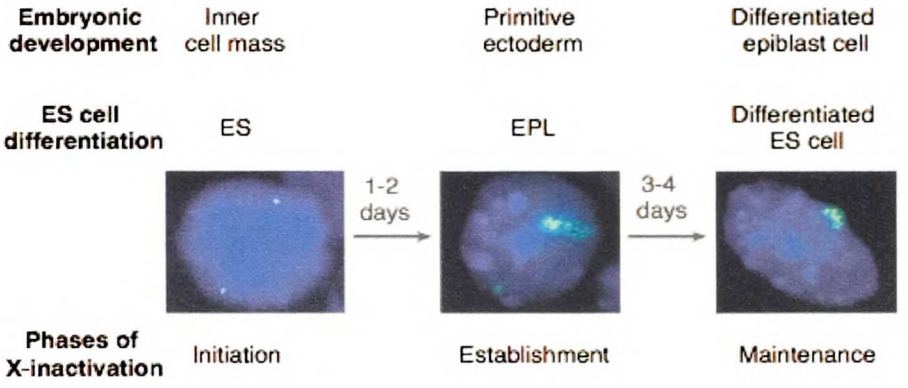
Embryonic development
Inner cell mass
Primitive ectoderm
Differentiated epiblast cell
ES cell differentiation
ES
EPL
Differentiated ES cell
1-2 days
3-4 days
Phases of X-inactivation
Initiation
Establishment
Maintenance

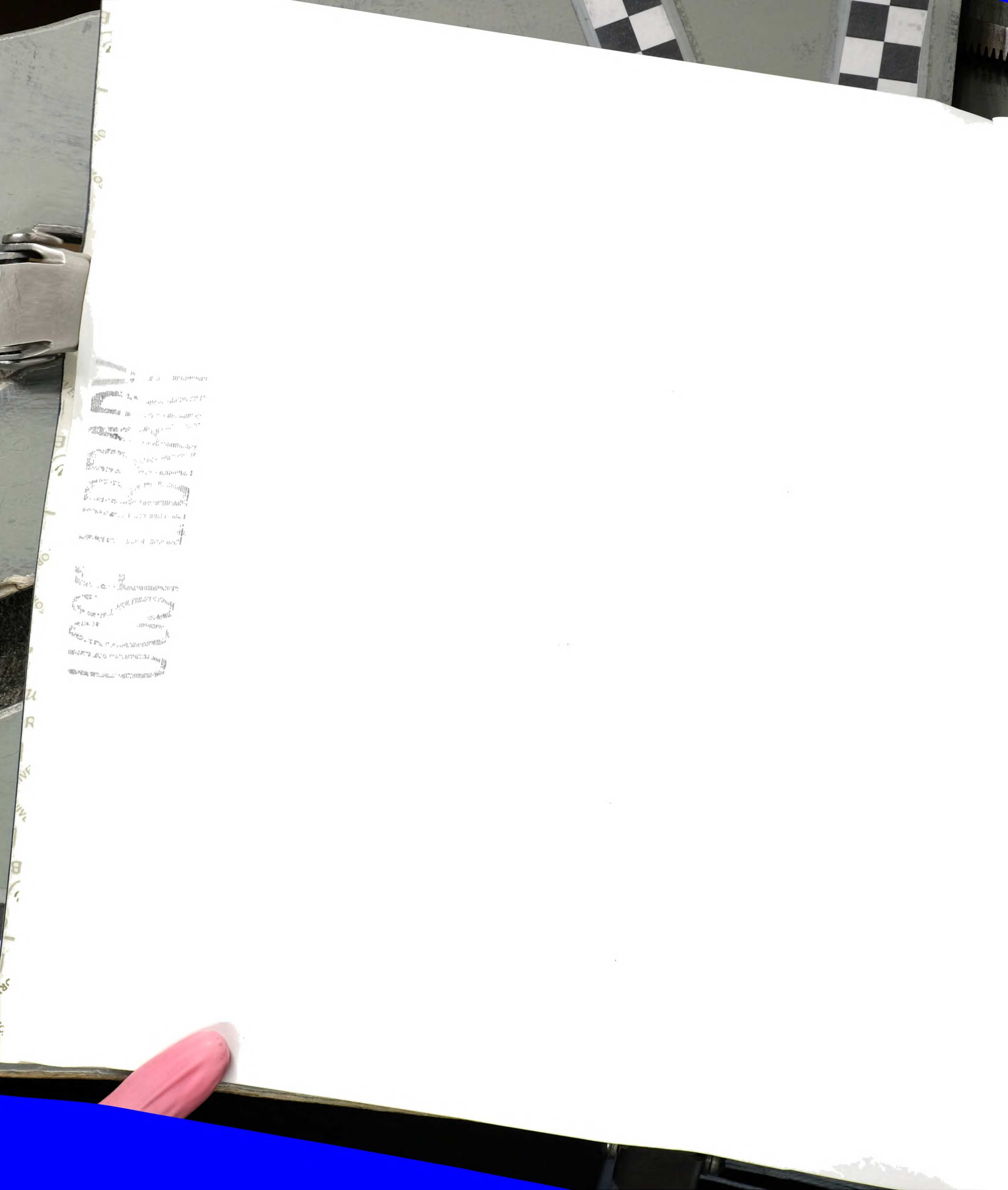

APPENDIX

Attempted lines of experimentation regarding SUZ12

In an attempt to further characterize the molecular role of SUZ12 in the SUV39H1 methylation system (discussed in Chapter 3), I attempted a number of experiments that were unsuccessful, inconclusive, or preliminary for a variety of reasons. They are outlined below:

1) SUZ12 immunoprecipitates H3-K9 HMTase activity

siRNA-mediated depletion of SUZ12 resulted in loss of H3-3mK9, suggesting that SUZ12 may be associated with H3-K9 HMTase activity. To address this hypothesis we performed immunoprecipitation experiments on cellular extracts expressing GFP-SUZ12, using a GFP antibody to immunoprecipitate GFP-SUZ12. Samples immunoprecipitated by anti-GFP from extracts expressing GFP-SUV39H1 only or rabbit IgG were used as positive and negative controls for HMTase activity. These immunoprecipitates were then applied to an in vitro HMTase assay, using an unmodified histone H3 N-terminal tail peptide or a pre-modified histone H3 N-terminal peptide with an acetyl modification at lysine 9 (H3-acK9) as the substrates (Figure 19). We found that the GFP-SUZ12 immunoprecipitate contained HMTase activity exclusively for the unmodified H3 peptide (Figure 19). This result indicates that SUZ12 co-immunoprecipitates of H3-K9 HMTase activity. This activity may be mediated through SUV39H1 or EZH2.

2) Identification of co-immunoprecipitated proteins via Mass Spectrometry

In collaboration with Feixia Chu, I performed an immunoprecipitation experiment for either GFP- tagged SUZ12 or GFP-tagged SUV39H1 and subjected the immunocomplexes to Mass Spectrometry analysis to identify co-immunoprecipitated proteins. EZH2 and EED were identified in the GFP-SUZ12 immunoprecipitates, and HP1a was identified in the GFP-SUV39H1 samples, indicating that the protocol worked well. However, SUV39H1 was not found in the GFP-SUZ12 immunoprecipitates, nor was SUZ12 found in the GFP-SUV39H1 immunoprecipitated samples. This suggests that interaction between SUZ12 and SUV39H1 may be transient.

3) Pull down experiments with recombinant SUV39H1 and SUZ12

Recombinant MBP-SUV39H1 was incubated with cell extracts overexpressing Myc-tagged SUZ12. *In vitro* binding assays using amylose- conjugated sepharose beads were performed. The precipitates were analyzed for presence of HP1α and Myc-tagged SUZ12 by Western Blotting. As expected, HP1α was specifically pulled down with MBP-SUV39H1 indicating that the recombinant protein was functional (Figure 20A). Myc-SUZ12 was enriched in the MBP-SUV39H1 samples when compared to MBP pull down (Figure 20B).

Conversely, binding assays were performed using doubly-tagged (GST at the N terminus and His at the C terminus) SUZ12 as the bait. Recombinant GST-SUZ12-His was incubated with extracts expressing GFP-SUV39H1. GFP-SVU39H1 was pulled down non-specifically with GST-SUZ12, as this protein was also present in GST only controls (data not shown). EZH2, a known SUZ12 partner, was not pulled down with recombinant SUZ12 (data not shown). It is possible that the presence of the His-tag at

the C-terminal end of SUZ12 disrupts proper folding of the protein or abrogates SUZ12 function. Future studies would include performing pull-downs using SUZ12 protein tagged only at the N-terminus.

4) Chromatin immunoprecipitation (ChIP) for SUV39H1, SUZ12, H3-3mK9 and H3-3mK27 at beta satellite repeats

I wished to determine if SUZ12 functions in maintaining the constitutive heterochromatin structure of pericentric regions by assaying for the presence of SUZ12 in those areas of the genome. To this end I performed ChIP for SUZ12, SUV3H1 and various histone modifications at beta satellite repeats, which are enriched at pericentric heterochromatin. H3-3mK9 and H3-3mK27 are clearly enriched on beta satellite repeats (Figure 21, lanes 7 and 8). In addition, it appears as though SUZ12 and EZH2 may be bound at beta satellites (Figure 21, lanes 5 and 9). SUV39H1 did not ChIP at levels above background (Figure 21, compare lane 6 with lanes 10 and 11), suggesting that SUV39H1 association at pericentric regions is transient. I probed SUZ12 and EZH2 chromatin immunocomplexes for presence at the *MYT* gene. This locus was previously shown to be bound by these two proteins and therefore served as a positive control for SUZ12 and EZH2 (Kirmizis *et al.*, 2004). The findings were confounded by the result that the positive control for SUZ12 and EZH2 did not work (data not shown). Neither of these proteins bound to the *MYT* locus. Because the appropriate control experiments were inconclusive, this line of experimentation was abandoned.

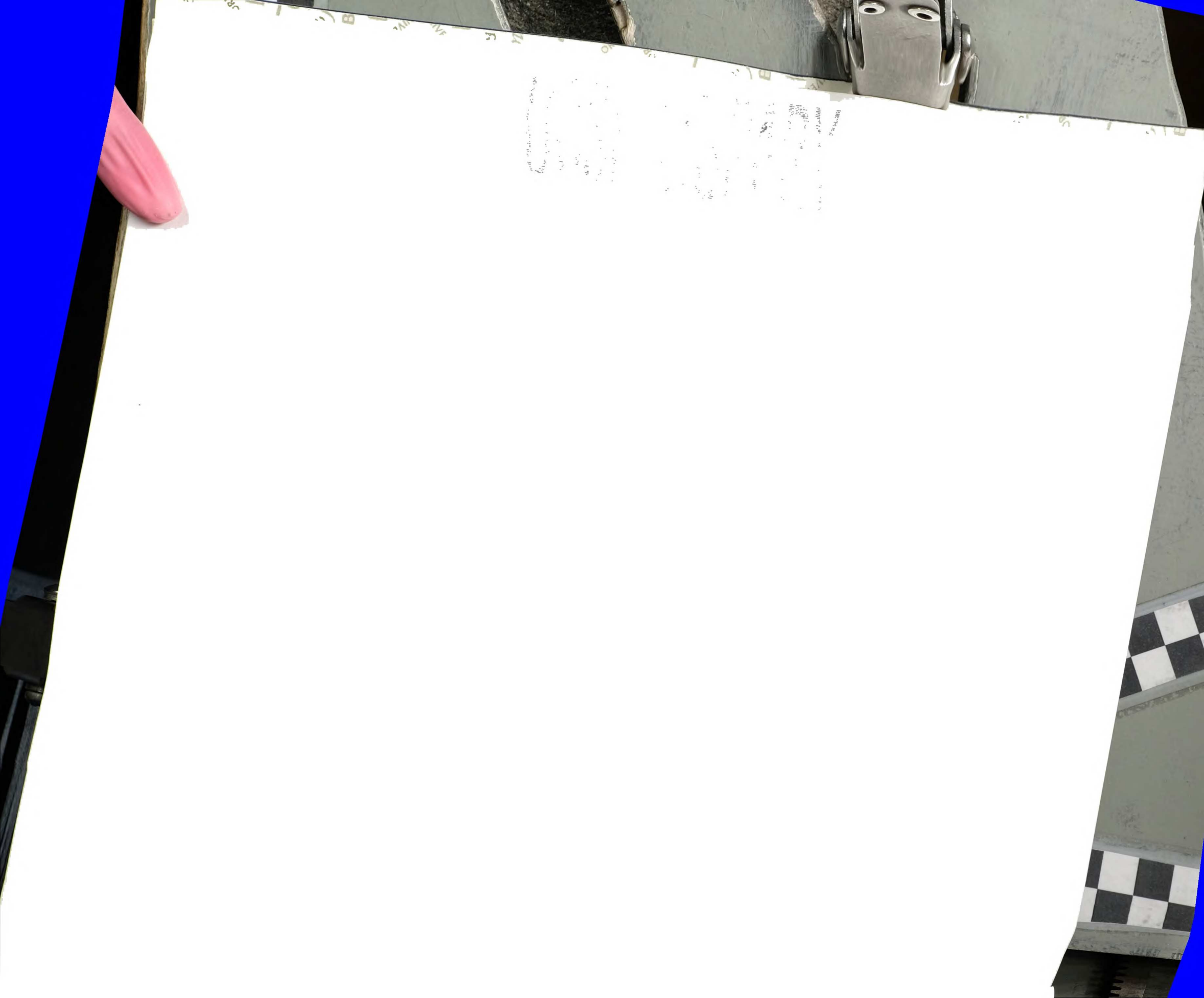

Materials and Methods

Co-Immunoprecipitation and HMTase assays

Forty-eight hours after transfection, HEK 293 cells were processed for co-immunoprecipitation as described, but in addition the cell extracts were treated with DNAse I (Worthington, 100 U/ml) for 15 minutes at 37 °C (Chu *et al.*, 2005). The immunoprecipitations were performed at 4 °C overnight. The resulting immunoprecipitates were then used for Western Blot analysis or subjected to HMTase assays essentially as described (Rea *et al.*, 2000). S-Adenosyl-L-(methyl-^{3}H) Methionine (74.0 Ci/nmol. Amersham) was used as the methyl donor and 5 ug of biotinylated N-terminal peptides were used as the substrate. The following peptides were used: wild-type N terminus of human histone H3 (ARTKQTARKSTGGK) and pre-modified peptide acetylated at K9 (modified residue is underlined) (ARTKQTARKacSTGGK). The peptides were kindly provided by Matthew D. Simon. After the HMTase assay, peptides were spotted onto SAM^2 Biotin Capture Membranes (Promega), washed, and subjected to scintillation counting as described (Patnaik *et al.*, 2004).

Mass Spectrometry

Mass spectrometric analysis of proteins was followed as outlined (Chu *et al.*, 2005).

MBP and GST *in vitro* binding assays

Human cDNA of SUV39H1 was cloned into the bacterial expression construct pMAL-c2X (NEB). Purification of MBP fusion proteins was performed as outlined by

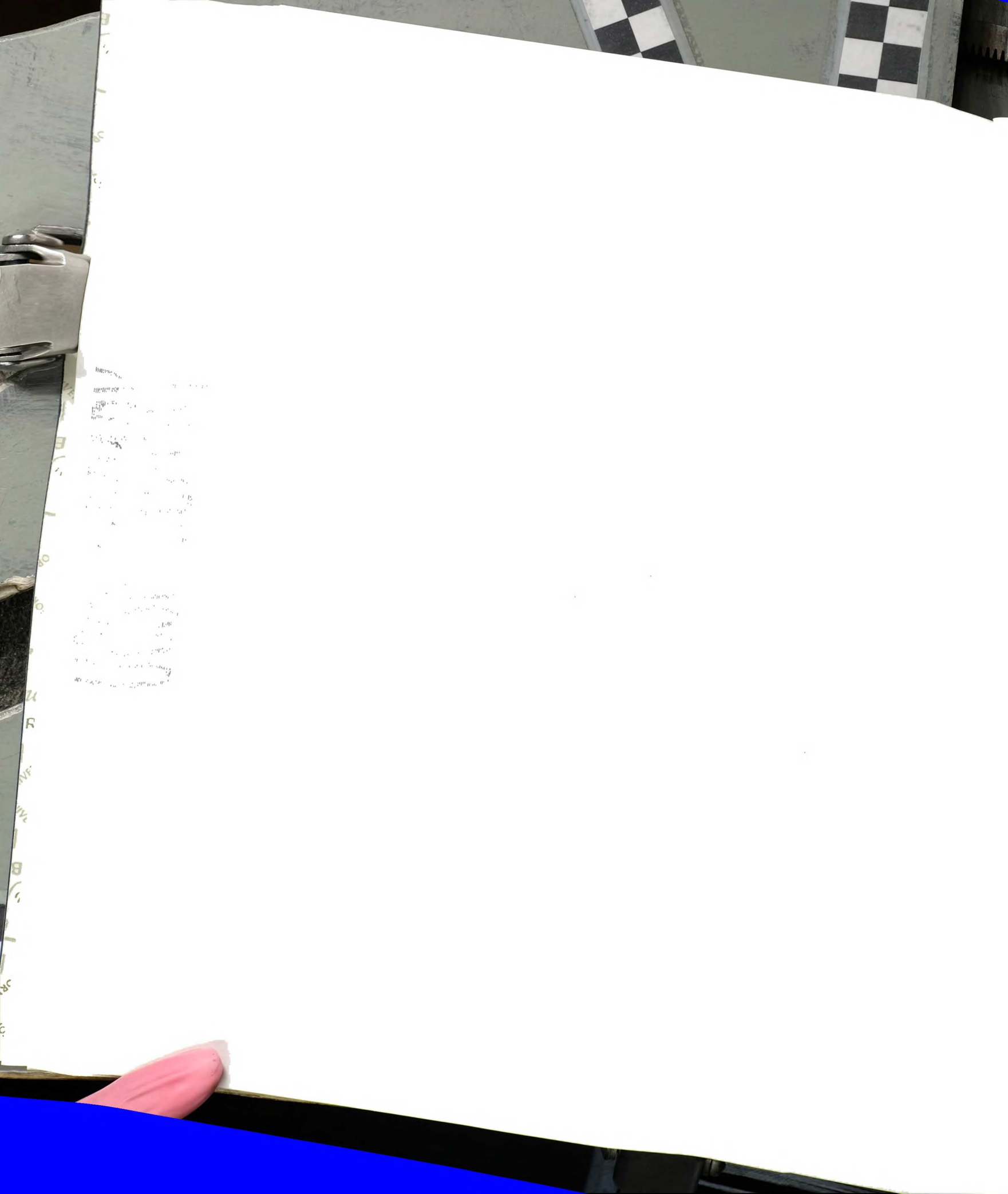

manufacturers instructions using amylose resin (NEB). The pull-down binding reaction was performed exactly as described (Tonozuka *et al.*, 2004), with the following alterations: 25ug of MBP-SUV39H1 or MBP was incubated with 1.5mg cellular extract for 2 hours at 4°C. Two washes were performed at 4°C , followed by 5 washes at room temperature using Ultrafree-MC filters (Millipore). The GST-SUZ12-HIS construct was created by inserting a 6x HIS tag into the 3' end of the SUZ12 cDNA. The resulting cDNA was then cloned into the bacterial expression plasmid pGEX-2T (Pharmacia Biotech). Tandem GST/HIS purification was performed in accordance with standard protocols using glutathione sepharose 4b beads (Amersham Biosciences) and BD TALON beads (BD Biosciences), respectively. GST pull-down experiments were performed as described (Yamamoto *et al.*, 2004), except that 25ug of immobilized fusion proteins was incubated with 1.5mg cellular extract. Antibodies used in western blotting were described in chapters 2 and 3. Two washes were performed at 4°C, followed by 5 washes at room temperature using Ultrafree-MC filters (Millipore).

Chromatin Immunoprecipitation

IMR90 cells were harvested and ChIP was performed exactly as outlined by (Kirmizis *et al.*, 2004), with the exception that protein A or protein G Dynabeads (Invitrogen) were used. Antibodies used for ChIP are detailed in chapters 2 and 3. PCR primers for the MYT locus are described (Kirmizis *et al.*, 2004) and beta satellite primers were taken from (Wang *et al.*, 2005).

Figure Legends

Figure 19. SUZ12 co-immunoprecipitates with H3-3mK9 HMTase activity. Peptides containing the first 14 amino acides of the H3 N-terminal tail (ARTKQTARKSTGGK) were methylated the GFP-SUZ12 immunocomplexes using tritiated SAM as the methyl donor. A peptide acetylaed at K9 served as a negative control. Ccounts incoporated were measured by filter- binding assay.

Figure 20. Association of SUZ12 and SUV39H1. (A) HP1α associates with MBP-SUV39H1 specifically (lane 3). (B) Cell extracts containing Myc-SUZ12 were incubated with either MBP-tagged SUV39H1 (lane 7) or MBP alone (lane 6). A control experiment was performed in which MBP-tagged SUV39H1 was incubated with non-transfected cell extract (lane 8). Myc-SUZ12 is specifically pulled-down by MBP-SUV39H1 (lane 7).

Figure 21. Chromatin immunoprecipitation at beta satellite repeats. ChIP experiments in IMR90 cells using antibodies to SUZ12 (lane 5), SUV39H1 (lane 6), H3-3mK9 (lane 7), H3-3mK27 (lane 8), EZH2 (lane 9), and a control IgG (lane 10). A control immunoprecipitation in which no antibody is used (lane 11). Dilutions of the total input are shown in lanes 1-4. Chromatin present in the immunocomplexes was analyzed with PCR using primers to beta satellites.

Figure 19

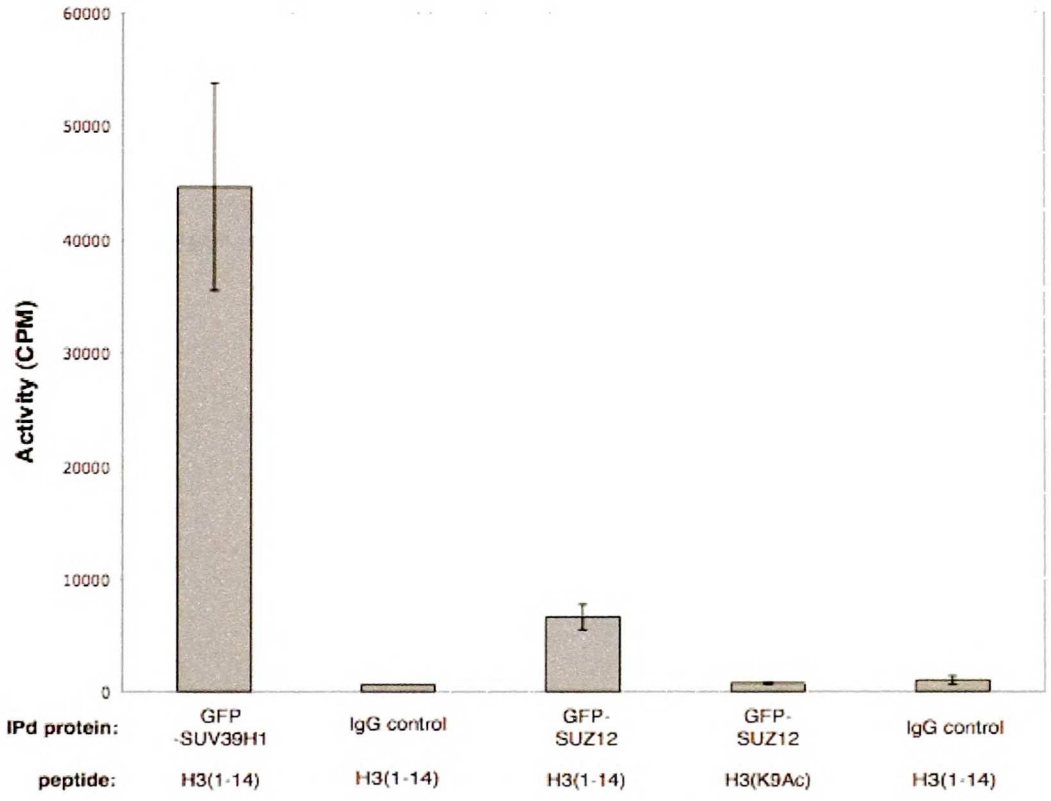
60000
50000
40000
30000
20000
10000
0
Activity (CPM)
IPd protein:
GFP -SUV39H1
IgG control
GFP-SUZ12
GFP-SUZ12
IgG control
peptide:
H3(1-14)
H3(1-14)
H3(1-14)
H3(K9Ac)
H3(1-14)

Figure 20

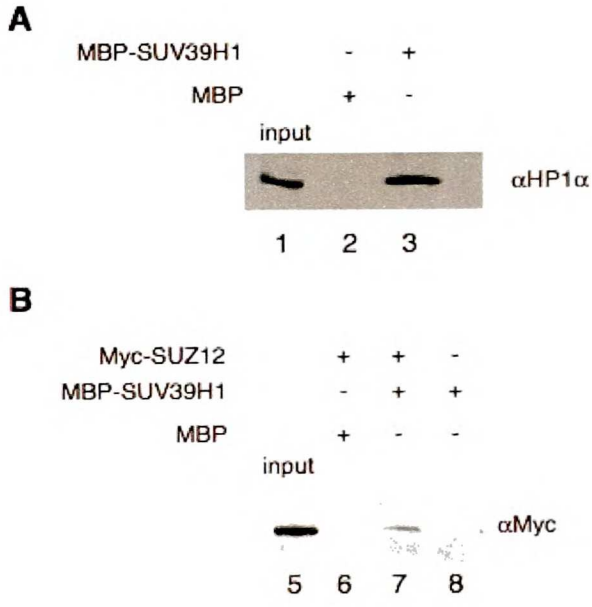
A
MBP-SUV39H1 - +
MBP + -
input
αHP1α
1 2 3
B
Myc-SUZ12 + + -
MBP-SUV39H1 - + +
MBP + - -
input
αMyc
5 6 7 8

Figure 21

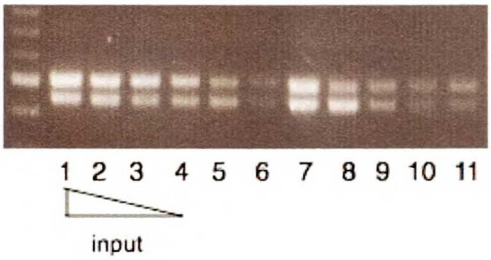

References

Aagaard, L., Laible, G., Selenko, P., Schmid, M., Dorn, R., Schotta, G., Kuhfittig, S., Wolf, A., Lebersorger, A., Singh, P.B., Reuter, G., and Jenuwein, T. (1999). Functional mammalian homologues of the Drosophila PEV-modifier Su(var)3-9 encode centromere-associated proteins which complex with the heterochromatin component M31. Embo J *18*, 1923-1938.

Bannister, A.J., Zegerman, P., Partridge, J.F., Miska, E.A., Thomas, J.O., Allshire, R.C., and Kouzarides, T. (2001). Selective recognition of methylated lysine 9 on histone H3 by the HP1 chromo domain. Nature *410*, 120-124.

Birve, A., Sengupta, A.K., Beuchle, D., Larsson, J., Kennison, J.A., Rasmuson-Lestander, A., and Muller, J. (2001). Su(z)12, a novel Drosophila Polycomb group gene that is conserved in vertebrates and plants. Development *128*, 3371-3379.

Breiling, A., O'Neill, L.P., D'Eliseo, D., Turner, B.M., and Orlando, V. (2004). Epigenome changes in active and inactive Polycomb-group-controlled regions. EMBO Rep *5*, 976-982.

Brook, F.A., and Gardner, R.L. (1997). The origin and efficient derivation of embryonic stem cells in the mouse. Proc Natl Acad Sci U S A *94*, 5709-5712.

Cao, R., Wang, L., Wang, H., Xia, L., Erdjument-Bromage, H., Tempst, P., Jones, R.S., and Zhang, Y. (2002). Role of histone H3 lysine 27 methylation in Polycomb-group silencing. Science *298*, 1039-1043.

Cao, R., and Zhang, Y. (2004a). The functions of E(Z)/EZH2-mediated methylation of lysine 27 in histone H3. Curr Opin Genet Dev *14*, 155-164.

Cao, R., and Zhang, Y. (2004b). SUZ12 Is Required for Both the Histone Methyltransferase Activity and the Silencing Function of the EED-EZH2 Complex. Mol Cell *15*, 57-67.

Chapman, G., Remiszewski, J.L., Webb, G.C., Schulz, T.C., Bottema, C.D., and Rathjen, P.D. (1997). The mouse homeobox gene, Gbx2: genomic organization and expression in pluripotent cells in vitro and in vivo. Genomics *46*, 223-233.

Chaumeil, J., Okamoto, I., Guggiari, M., and Heard, E. (2002). Integrated kinetics of X chromosome inactivation in differentiating embryonic stem cells. Cytogenet Genome Res *99*, 75-84.

Cheutin, T., McNairn, A.J., Jenuwein, T., Gilbert, D.M., Singh, P.B., and Misteli, T. (2003). Maintenance of stable heterochromatin domains by dynamic HP1 binding. Science *299*, 721-725.

Chu, F., Nusinow, D.A., Chalkley, R.J., Plath, K., Panning, B., and Burlingame, A.L. (2005). Mapping post-translational modifications of the histone variant macroH2A1 using tandem mass spectrometry. Mol Cell Proteomics.

Cohen, H.R., Royce-Tolland, M.E., Worringer, K.A., and Panning, B. (2005). Chromatin modifications on the inactive X chromosome. Prog Mol Subcell Biol *38*, 91-122.

Coucouvanis, E., and Martin, G.R. (1995). Signals for death and survival: a two-step mechanism for cavitation in the vertebrate embryo. Cell *83*, 279-287.

Coucouvanis, E., and Martin, G.R. (1999). BMP signaling plays a role in visceral endoderm differentiation and cavitation in the early mouse embryo. Development *126*, 535-546.
Czermin, B., Melfi, R., McCabe, D., Seitz, V., Imhof, A., and Pirrotta, V. (2002). Drosophila enhancer of Zeste/ESC complexes have a histone H3 methyltransferase activity that marks chromosomal Polycomb sites. Cell *111*, 185-196.
de la Cruz, C.C., Fang, J., Plath, K., Worringer, K.A., Nusinow, D.A., Zhang, Y., and Panning, B. (2005). Developmental regulation of Suz 12 localization. Chromosoma *114*, 183-192.
de Napoles, M., Mermoud, J.E., Wakao, R., Tang, Y.A., Endoh, M., Appanah, R., Nesterova, T.B., Silva, J., Otte, A.P., Vidal, M., Koseki, H., and Brockdorff, N. (2004). Polycomb group proteins Ring1A/B link ubiquitylation of histone H2A to heritable gene silencing and X inactivation. Dev Cell *7*, 663-676.
Erhardt, S., Su, I.H., Schneider, R., Barton, S., Bannister, A.J., Perez-Burgos, L., Jenuwein, T., Kouzarides, T., Tarakhovsky, A., and Surani, M.A. (2003). Consequences of the depletion of zygotic and embryonic enhancer of zeste 2 during preimplantation mouse development. Development *130*, 4235-4248.
Fang, J., Chen, T., Chadwick, B., Li, E., and Zhang, Y. (2004). Ring1b-mediated H2A ubiquitination associates with inactive X chromosomes and is involved in Initiation of X-inactivation. J Biol Chem.
Festenstein, R., Pagakis, S.N., Hiragami, K., Lyon, D., Verreault, A., Sekkali, B., and Kioussis, D. (2003). Modulation of heterochromatin protein 1 dynamics in primary Mammalian cells. Science *299*, 719-721.
Garcia-Cao, M., O'Sullivan, R., Peters, A.H., Jenuwein, T., and Blasco, M.A. (2004). Epigenetic regulation of telomere length in mammalian cells by the Suv39h1 and Suv39h2 histone methyltransferases. Nat Genet *36*, 94-99.
Gardner, R.L., and Lyon, M.F. (1971). X chromosome inactivation studied by injection of a single cell into the mouse blastocyst. Nature *231*, 385-386.
Gardner, R.L., and Rossant, J. (1979). Investigation of the fate of 4-5 day post-coitum mouse inner cell mass cells by blastocyst injection. J Embryol Exp Morphol *52*, 141-152.
Gilbert, N., Boyle, S., Sutherland, H., de Las Heras, J., Allan, J., Jenuwein, T., and Bickmore, W.A. (2003). Formation of facultative heterochromatin in the absence of HP1. Embo J *22*, 5540-5550.
Goto, T., and Monk, M. (1998). Regulation of X-chromosome inactivation in development in mice and humans. Microbiol Mol Biol Rev *62*, 362-378.
Grewal, S.I., and Moazed, D. (2003). Heterochromatin and epigenetic control of gene expression. Science *301*, 798-802.
Hall, I.M., Shankaranarayana, G.D., Noma, K., Ayoub, N., Cohen, A., and Grewal, S.I. (2002). Establishment and maintenance of a heterochromatin domain. Science *297*, 2232-2237.
Hamer, K.M., Sewalt, R.G., den Blaauwen, J.L., Hendrix, T., Satijn, D.P., and Otte, A.P. (2002). A panel of monoclonal antibodies against human polycomb group proteins. Hybrid Hybridomics *21*, 245-252.
Haub, O., and Goldfarb, M. (1991). Expression of the fibroblast growth factor-5 gene in the mouse embryo. Development *112*, 397-406.

Hayakawa, T., Haraguchi, T., Masumoto, H., and Hiraoka, Y. (2003). Cell cycle behavior of human HP1 subtypes: distinct molecular domains of HP1 are required for their centromeric localization during interphase and metaphase. J Cell Sci *116*, 3327-3338.
Heard, E. (2004). Recent advances in X-chromosome inactivation. Curr Opin Cell Biol *16*, 247-255.
Hoffelder, D.R., Luo, L., Burke, N.A., Watkins, S.C., Gollin, S.M., and Saunders, W.S. (2004). Resolution of anaphase bridges in cancer cells. Chromosoma *112*, 389-397.
Jallepalli, P.V., and Lengauer, C. (2001). Chromosome segregation and cancer: cutting through the mystery. Nat Rev Cancer *1*, 109-117.
Jenuwein, T., and Allis, C.D. (2001). Translating the histone code. Science *293*, 1074-1080.
Ketel, C.S., Andersen, E.F., Vargas, M.L., Suh, J., Strome, S., and Simon, J.A. (2005). Subunit contributions to histone methyltransferase activities of fly and worm polycomb group complexes. Mol Cell Biol *25*, 6857-6868.
Kirmizis, A., Bartley, S.M., and Farnham, P.J. (2003). Identification of the polycomb group protein SU(Z)12 as a potential molecular target for human cancer therapy. Mol Cancer Ther *2*, 113-121.
Kirmizis, A., Bartley, S.M., Kuzmichev, A., Margueron, R., Reinberg, D., Green, R., and Farnham, P.J. (2004). Silencing of human polycomb target genes is associated with methylation of histone H3 Lys 27. Genes Dev *18*, 1592-1605.
Kunath, T., Strumpf, D., and Rossant, J. (2004). Early trophoblast determination and stem cell maintenance in the mouse--a review. Placenta *25 Suppl A*, S32-38.
Kuzmichev, A., Jenuwein, T., Tempst, P., and Reinberg, D. (2004). Different EZH2-containing complexes target methylation of histone H1 or nucleosomal histone H3. Mol Cell *14*, 183-193.
Kuzmichev, A., Margueron, R., Vaquero, A., Preissner, T.S., Scher, M., Kirmizis, A., Ouyang, X., Brockdorff, N., Abate-Shen, C., Farnham, P., and Reinberg, D. (2005). Composition and histone substrates of polycomb repressive group complexes change during cellular differentiation. Proc Natl Acad Sci U S A *102*, 1859-1864.
Kuzmichev, A., Nishioka, K., Erdjument-Bromage, H., Tempst, P., and Reinberg, D. (2002). Histone methyltransferase activity associated with a human multiprotein complex containing the Enhancer of Zeste protein. Genes Dev *16*, 2893-2905.
Lachner, M., O'Carroll, D., Rea, S., Mechtler, K., and Jenuwein, T. (2001). Methylation of histone H3 lysine 9 creates a binding site for HP1 proteins. Nature *410*, 116-120.
Lehnertz, B., Ueda, Y., Derijck, A.A., Braunschweig, U., Perez-Burgos, L., Kubicek, S., Chen, T., Li, E., Jenuwein, T., and Peters, A.H. (2003). Suv39h-mediated histone H3 lysine 9 methylation directs DNA methylation to major satellite repeats at pericentric heterochromatin. Curr Biol *13*, 1192-1200.
Maison, C., Bailly, D., Peters, A.H., Quivy, J.P., Roche, D., Taddei, A., Lachner, M., Jenuwein, T., and Almouzni, G. (2002). Higher-order structure in pericentric heterochromatin involves a distinct pattern of histone modification and an RNA component. Nat Genet *30*, 329-334.
Mak, W., Baxter, J., Silva, J., Newall, A.E., Otte, A.P., and Brockdorff, N. (2002). Mitotically stable association of polycomb group proteins eed and enx1 with the inactive x chromosome in trophoblast stem cells. Curr Biol *12*, 1016-1020.

Marahrens, Y., Panning, B., Dausman, J., Strauss, W., and Jaenisch, R. (1997). Xist-deficient mice are defective in dosage compensation but not spermatogenesis. Genes Dev *11*, 156-166.
Melcher, M., Schmid, M., Aagaard, L., Selenko, P., Laible, G., and Jenuwein, T. (2000). Structure-function analysis of SUV39H1 reveals a dominant role in heterochromatin organization, chromosome segregation, and mitotic progression. Mol Cell Biol *20*, 3728-3741.
Minc, E., Allory, Y., Worman, H.J., Courvalin, J.C., and Buendia, B. (1999). Localization and phosphorylation of HP1 proteins during the cell cycle in mammalian cells. Chromosoma *108*, 220-234.
Monk, M., and Harper, M.I. (1979). Sequential X chromosome inactivation coupled with cellular differentiation in early mouse embryos. Nature *281*, 311-313.
Muller, J., Hart, C.M., Francis, N.J., Vargas, M.L., Sengupta, A., Wild, B., Miller, E.L., O'Connor, M.B., Kingston, R.E., and Simon, J.A. (2002). Histone methyltransferase activity of a Drosophila Polycomb group repressor complex. Cell *111*, 197-208.
Nakayama, J., Rice, J.C., Strahl, B.D., Allis, C.D., and Grewal, S.I. (2001). Role of histone H3 lysine 9 methylation in epigenetic control of heterochromatin assembly. Science *292*, 110-113.
Nekrasov, M., Wild, B., and Muller, J. (2005). Nucleosome binding and histone methyltransferase activity of Drosophila PRC2. EMBO Rep *6*, 348-353.
Neubuser, A., Peters, H., Balling, R., and Martin, G.R. (1997). Antagonistic interactions between FGF and BMP signaling pathways: a mechanism for positioning the sites of tooth formation. Cell *90*, 247-255.
Nielsen, A.L., Oulad-Abdelghani, M., Ortiz, J.A., Remboutsika, E., Chambon, P., and Losson, R. (2001). Heterochromatin formation in mammalian cells: interaction between histones and HP1 proteins. Mol Cell *7*, 729-739.
Pal-Bhadra, M., Leibovitch, B.A., Gandhi, S.G., Rao, M., Bhadra, U., Birchler, J.A., and Elgin, S.C. (2004). Heterochromatic silencing and HP1 localization in Drosophila are dependent on the RNAi machinery. Science *303*, 669-672.
Panning, B., Dausman, J., and Jaenisch, R. (1997). X chromosome inactivation is mediated by Xist RNA stabilization. Cell *90*, 907-916.
Pasini, D., Bracken, A.P., Jensen, M.R., Denchi, E.L., and Helin, K. (2004). Suz12 is essential for mouse development and for EZH2 histone methyltransferase activity. Embo J.
Patnaik, D., Chin, H.G., Esteve, P.O., Benner, J., Jacobsen, S.E., and Pradhan, S. (2004). Substrate specificity and kinetic mechanism of mammalian G9a histone H3 methyltransferase. J Biol Chem *279*, 53248-53258.
Penny, G.D., Kay, G.F., Sheardown, S.A., Rastan, S., and Brockdorff, N. (1996). Requirement for Xist in X chromosome inactivation. Nature *379*, 131-137.
Peters, A.H., Kubicek, S., Mechtler, K., O'Sullivan, R.J., Derijck, A.A., Perez-Burgos, L., Kohlmaier, A., Opravil, S., Tachibana, M., Shinkai, Y., Martens, J.H., and Jenuwein, T. (2003). Partitioning and plasticity of repressive histone methylation states in mammalian chromatin. Mol Cell *12*, 1577-1589.
Peters, A.H., O'Carroll, D., Scherthan, H., Mechtler, K., Sauer, S., Schofer, C., Weipoltshammer, K., Pagani, M., Lachner, M., Kohlmaier, A., Opravil, S., Doyle, M.,

Sibilia, M., and Jenuwein, T. (2001). Loss of the Suv39h histone methyltransferases impairs mammalian heterochromatin and genome stability. Cell *107*, 323-337.
Plath, K., Fang, J., Mlynarczyk-Evans, S.K., Cao, R., Worringer, K.A., Wang, H., de la Cruz, C.C., Otte, A.P., Panning, B., and Zhang, Y. (2003). Role of histone H3 lysine 27 methylation in X inactivation. Science *300*, 131-135.
Plath, K., Mlynarczyk-Evans, S., Nusinow, D.A., and Panning, B. (2002). Xist RNA and the mechanism of X chromosome inactivation. Annu Rev Genet *36*, 233-278.
Plath, K., Talbot, D., Hamer, K.M., Otte, A.P., Yang, T.P., Jaenisch, R., and Panning, B. (2004). Developmentally regulated alterations in Polycomb repressive complex 1 proteins on the inactive X chromosome. J Cell Biol.
Rathjen, J., Lake, J.A., Bettess, M.D., Washington, J.M., Chapman, G., and Rathjen, P.D. (1999). Formation of a primitive ectoderm like cell population, EPL cells, from ES cells in response to biologically derived factors. J Cell Sci *112 (Pt 5)*, 601-612.
Rea, S., Eisenhaber, F., O'Carroll, D., Strahl, B.D., Sun, Z.W., Schmid, M., Opravil, S., Mechtler, K., Ponting, C.P., Allis, C.D., and Jenuwein, T. (2000). Regulation of chromatin structure by site-specific histone H3 methyltransferases. Nature *406*, 593-599.
Reuter, G., and Wolff, I. (1981). Isolation of dominant suppressor mutations for position-effect variegation in Drosophila melanogaster. Mol Gen Genet *182*, 516-519.
Rice, J.C., Briggs, S.D., Ueberheide, B., Barber, C.M., Shabanowitz, J., Hunt, D.F., Shinkai, Y., and Allis, C.D. (2003). Histone methyltransferases direct different degrees of methylation to define distinct chromatin domains. Mol Cell *12*, 1591-1598.
Rogers, M.B., Hosler, B.A., and Gudas, L.J. (1991). Specific expression of a retinoic acid-regulated, zinc-finger gene, Rex-1, in preimplantation embryos, trophoblast and spermatocytes. Development *113*, 815-824.
Sheardown, S.A., Newall, A.E., Norris, D.P., Rastan, S., and Brockdorff, N. (1997). Regulatory elements in the minimal promoter region of the mouse Xist gene. Gene *203*, 159-168.
Silva, J., Mak, W., Zvetkova, I., Appanah, R., Nesterova, T.B., Webster, Z., Peters, A.H., Jenuwein, T., Otte, A.P., and Brockdorff, N. (2003). Establishment of histone h3 methylation on the inactive X chromosome requires transient recruitment of Eed-Enx1 polycomb group complexes. Dev Cell *4*, 481-495.
Sinclair, D.A., Lloyd, V.K., and Grigliatti, T.A. (1989). Characterization of mutations that enhance position-effect variegation in Drosophila melanogaster. Mol Gen Genet *216*, 328-333.
Smith, K.P., Byron, M., Clemson, C.M., and Lawrence, J.B. (2004). Ubiquitinated proteins including uH2A on the human and mouse inactive X chromosome: enrichment in gene rich bands. Chromosoma *113*, 324-335.
Taddei, A., Maison, C., Roche, D., and Almouzni, G. (2001). Reversible disruption of pericentric heterochromatin and centromere function by inhibiting deacetylases. Nat Cell Biol *3*, 114-120.
Takagi, N., Sugawara, O., and Sasaki, M. (1982). Regional and temporal changes in the pattern of X-chromosome replication during the early post-implantation development of the female mouse. Chromosoma *85*, 275-286.
Tan, S.S., Williams, E.A., and Tam, P.P. (1993). X-chromosome inactivation occurs at different times in different tissues of the post-implantation mouse embryo. Nat Genet *3*, 170-174.

Tanaka, S., Kunath, T., Hadjantonakis, A.K., Nagy, A., and Rossant, J. (1998). Promotion of trophoblast stem cell proliferation by FGF4. Science *282*, 2072-2075.
Tonozuka, Y., Minoshima, Y., Bao, Y.C., Moon, Y., Tsubono, Y., Hatori, T., Nakajima, H., Nosaka, T., Kawashima, T., and Kitamura, T. (2004). A GTPase-activating protein binds STAT3 and is required for IL-6-induced STAT3 activation and for differentiation of a leukemic cell line. Blood *104*, 3550-3557.
Uy, G.D., Downs, K.M., and Gardner, R.L. (2002). Inhibition of trophoblast stem cell potential in chorionic ectoderm coincides with occlusion of the ectoplacental cavity in the mouse. Development *129*, 3913-3924.
Volpe, T., Schramke, V., Hamilton, G.L., White, S.A., Teng, G., Martienssen, R.A., and Allshire, R.C. (2003). RNA interference is required for normal centromere function in fission yeast. Chromosome Res *11*, 137-146.
Volpe, T.A., Kidner, C., Hall, I.M., Teng, G., Grewal, S.I., and Martienssen, R.A. (2002). Regulation of heterochromatic silencing and histone H3 lysine-9 methylation by RNAi. Science *297*, 1833-1837.
Wang, J., Mager, J., Chen, Y., Schneider, E., Cross, J.C., Nagy, A., and Magnuson, T. (2001). Imprinted X inactivation maintained by a mouse Polycomb group gene. Nat Genet *28*, 371-375.
Wang, Q., Zhang, Z., Blackwell, K., and Carmichael, G.G. (2005). Vigilins bind to promiscuously A-to-I-edited RNAs and are involved in the formation of heterochromatin. Curr Biol *15*, 384-391.
Wutz, A., and Jaenisch, R. (2000). A shift from reversible to irreversible X inactivation is triggered during ES cell differentiation. Mol Cell *5*, 695-705.
Wutz, A., Rasmussen, T.P., and Jaenisch, R. (2002). Chromosomal silencing and localization are mediated by different domains of Xist RNA. Nat Genet *30*, 167-174.
Yamamoto, K., and Sonoda, M. (2003). Self-interaction of heterochromatin protein 1 is required for direct binding to histone methyltransferase, SUV39H1. Biochem Biophys Res Commun *301*, 287-292.
Yamamoto, K., Sonoda, M., Inokuchi, J., Shirasawa, S., and Sasazuki, T. (2004). Polycomb group suppressor of zeste 12 links heterochromatin protein 1alpha and enhancer of zeste 2. J Biol Chem *279*, 401-406.

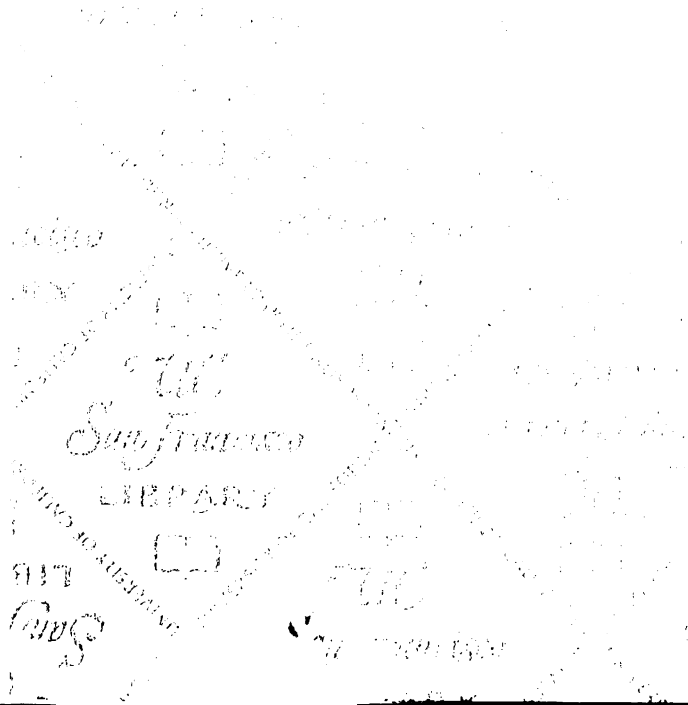
The
San Francisco
LIBRARY